High-throughput descriptors in materials development

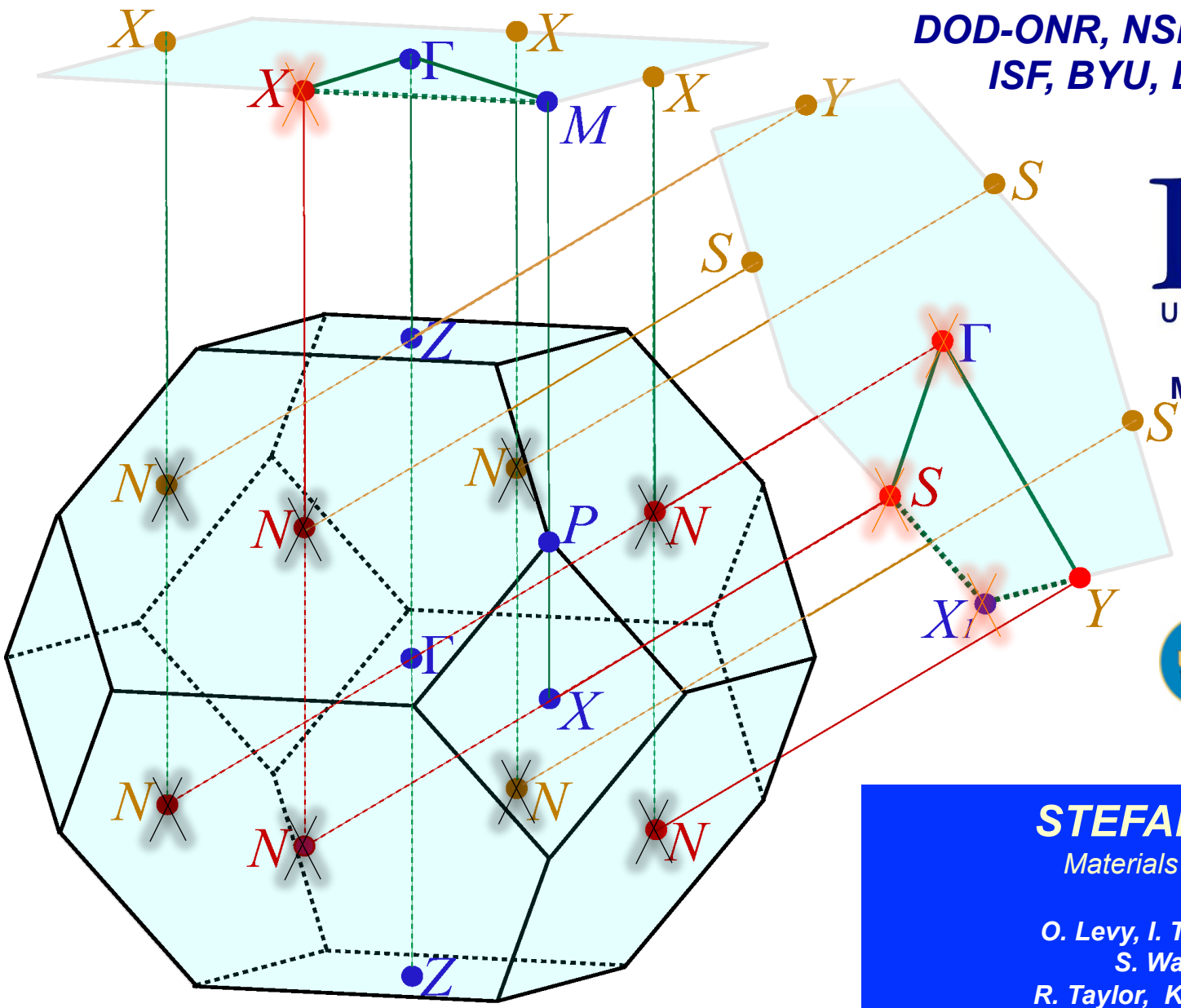

DOD-ONR, NSF, DOE, DHS, NIST, ISF, BYU, DOD-MURI, Boeing

Duke UNIVERSITY

CENTER *for* MATERIALS GENOMICS

STEFANO CURTAROLO

*Materials Science - **Duke University***

O. Levy, I. Takeuchi, G. Hart, J. Carrete, S. Wang, M. Buongiorno Nardelli, R. Taylor, K. Yang, N. Mingo, S. Sanvito

COMPUTATIONAL MATERIALS GENOME

procedures of synthesis. Is there another way? Indeed, this is the burgeoning area of computational materials science called 'high-throughput' (HT) computational materials design. It is based on the marriage between computational quantum-mechanical–thermodynamic approaches[1,2] and a multitude of techniques rooted in database construction and intelligent data mining[3]. The concept is simple yet powerful: create a large database containing the calculated thermodynamic and electronic properties of existing and hypothetical materials, and then intelligently interrogate the database in the search of materials with the desired properties. Clearly, the entire construct should be validated by reality, namely the existing materials must be predicted correctly and the hypothetical ones should eventually be made. Such a reality check feeds back to the power.

nature materials

REVIEW ARTICLE

PUBLISHED ONLINE: 20 FEBRUARY 2013 | DOI: 10.1038/NMAT3568

The high-throughput highway to computational materials design

Curtarolo*, Hart, Buongiorno Nardelli, Mingo, Sanvito, Levy

DOI: 10.1038/NMAT3568 (March 2013)

COMPUTATIONAL High-Throughput

The practical implementation of computational HT is highly non-trivial. The method is employed in three strictly connected steps: (i) virtual materials growth: thermodynamic and electronic structure calculations of materials[3,23]; (ii) rational materials storage: systematic storage of the information in database repositories[24,25]; (iii) materials characterization and selection: data analysis aimed at selecting novel materials or gaining new physical insights[15,19,26].

nature materials

REVIEW ARTICLE

PUBLISHED ONLINE: 20 FEBRUARY 2013 | DOI: 10.1038/NMAT3568

The high-throughput highway to computational materials design

Curtarolo*, Hart, Buongiorno Nardelli, Mingo, Sanvito, Levy

DOI: 10.1038/NMAT3568 (March 2013)

MATERIALS GENOME: genes+descriptors

Table 1 | Examples of descriptors introduced in the literature. Nature Mater. **12**, 191 (2013)

Problem	Combination of materials properties (gene)	Descriptor
Structure stability: convex hull of an alloy system	Formation enthalpy (H_f) as a function of concentration (x) and the enthalpies (H) of A and B.	$H_f(x) = H(A_{1-x}B_x) - (1-x)H(A) - xH(B)$
Phase stability in off-lattice alloys PRL **91**, 135503 (2003)	Spectral decomposition of alloy vector-energies ($E_{n,p}$, n-rows = species, p-columns = configurations) with principal-component-analysis coefficients (α	$E_{n,p} \simeq \alpha_1 E_{n,1} + \cdots + \alpha_{p-1} E_{n,p-1} + \epsilon(d)$
Nano… PR…	Ratio of the av… (ref. 15).	
Topol… Nat…	Variational rat… derivative stra… k, a_0 lattice)[16].	…rbit …at
Powe… (spec… …cy) PRL **108**, 068701 (2012)	Ratio of the m… energy density… recombinatio… …E)) — versus bandgap energy (E_g)[62].	…ident solar …on–hole
Non-proportionality in scintillators IEEE Trans. Nucl. Sci. **56**, 2989 (2009)	Maximum mismatch between effective masses of electrons (m_e) and holes (m_h)[75].	$\hat{\chi}_{np} \equiv \max\left(\frac{m_e}{m_h}, \frac{m_h}{m_e}\right)$
Morphotropic phase boundary piezoelectrics PRB **84**, 014103 (2011)	Energy proximity between tetragonal, rhombohedra and rotational distortions (ΔE_p). Angular coordinate (α_{AB}) of the energy minimum in the A–B off-centerings energy map for ABO_3 systems[79].	$\Delta E_p \leq 0.5$ eV $\alpha_{AB} \approx 45°$

the "problem"

qualitative picture

quantitative picture

The automatism is all about creating a big picture from to too many small details

Lycurgus cup (290~325 AD) AgAu NP~10nm
dichroism by resonant surface plasmon

NEED fast standards

Calculate electronic structure of all reported compounds

- *ICSD ~150,000 (well defined ~50%)*
- *Work out all the prototype definitions/symmetries:*
- *Define standards in reciprocal space (on-line):*

a highly complex solution to an apparently simple problem

- *Obtain LDAU parameters when required*
- *Adiabatic U* $E[U] = \int_0^{\{U\}} \delta E/\delta U_i \cdot dU_i$
- *Automatic switch to LS coupling when required*
- *Calculate stability, if necessary*
- *Discover properties through correlations*
- *Make ONLINE Tools*
- *Use results as* ***STARTING POINTS***
- *Works for VASP and QE*

Algorithm has 25 self consistent points

$$(\mathbf{a}_1, \mathbf{a}_2, \mathbf{a}_3)_{BL}^{n+1} = \mathrm{Dual}\left[\mathrm{Minkowski}_{BL^*}\left[\mathrm{Dual}\left[(\mathbf{a}_1, \mathbf{a}_2, \mathbf{a}_3)_{BL}^{n}\right]\right]\right]$$

14 Bravais Lattices ➔ 25 Brillouin Zones ➔ 25 Bravais Definitions

CUBIC: cub, bcc, fcc
TETRAGONAL: tet, bct_1, bct_2
ORTHORHOMBIC: orc, $orcf_1$, $orcf_2$, $orcf_2$, orci, orcc
HEXAGONAL/TRIGONAL: hex, rhl_1, rhl_2
MONOCLINIC: mcl, $mclc_1$, $mclc_2$, $mclc_3$, $mclc_4$, $mclc_5$
TRICLINIC: tri_{1a}, tri_{2a}, tri_{1b}, tri_{2b}

materials.duke.edu/awrapper.html
High-throughput electronic structure calculations: Comp. Mat. Sci. ***49****, 299-312 (2010)*

STANDARD in Real Space and Reciprocal Space

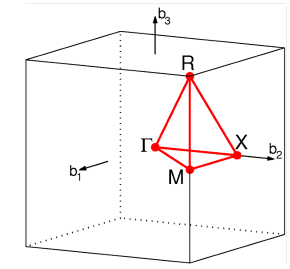

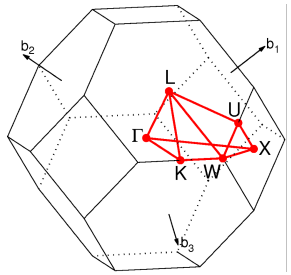

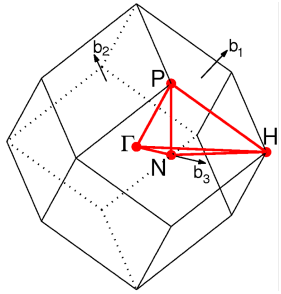

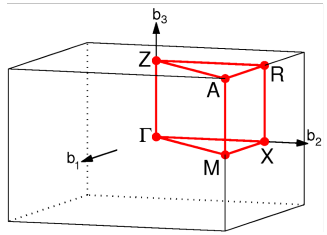

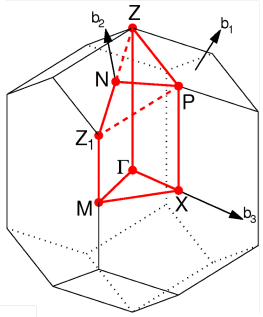

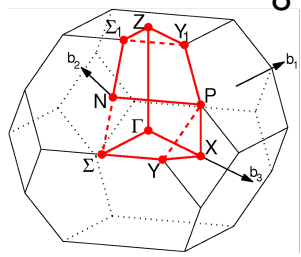

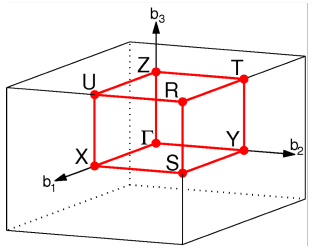

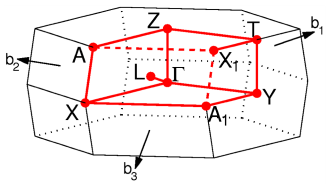

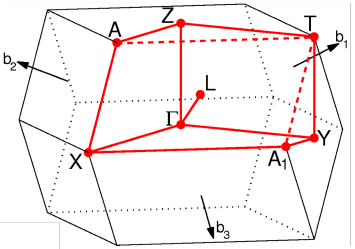

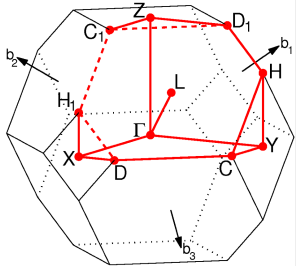

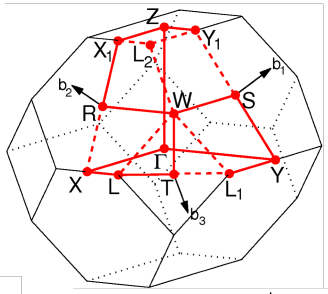

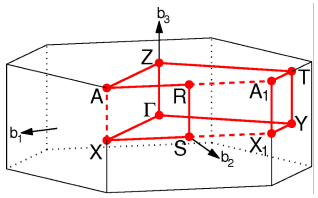

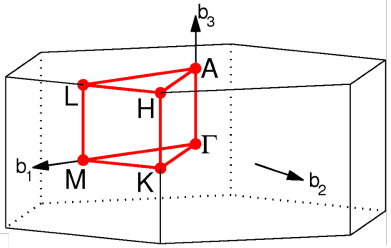

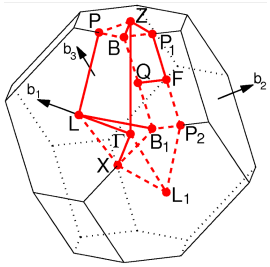

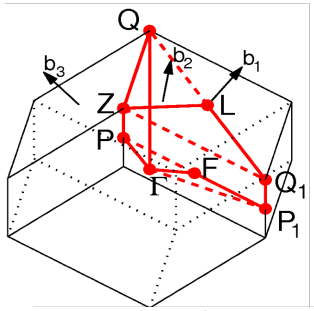

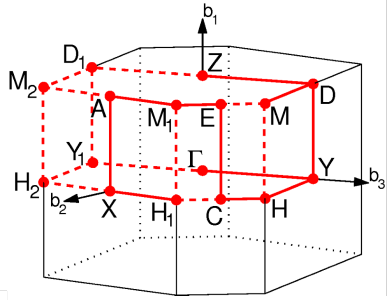

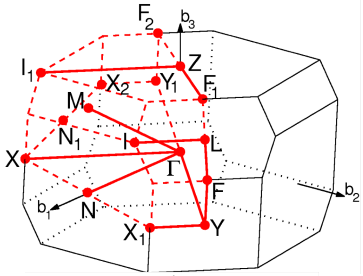

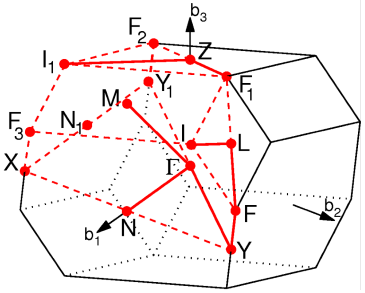

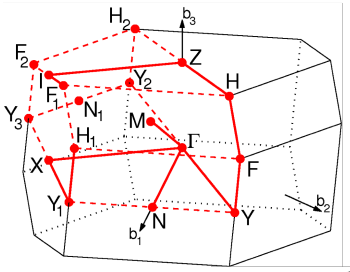

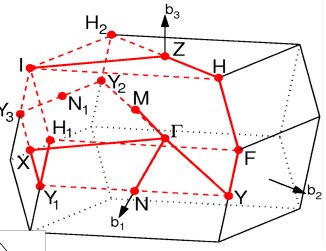

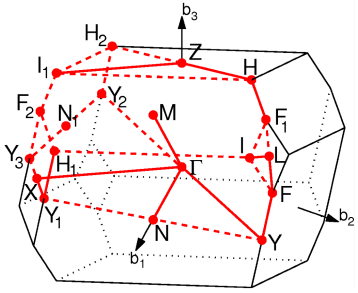

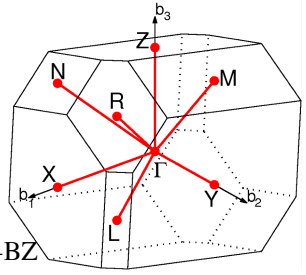

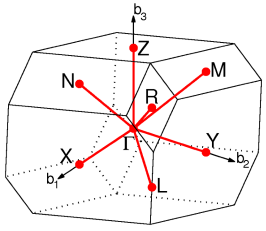

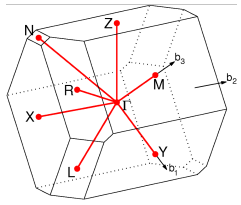

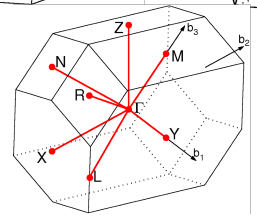

.. after 25 cases
and 1000 online headaches … A

Repository of quantum mechanics calculations

AFLOW framework libraries: www.aflowlib.org
Online/socket commands for the SQL database interrogation.
Distributed platform will work on Linux/UNIX platforms

Duke UNIVERSITY CENTER *for* MATERIALS GENOMICS

(a)

AFLOWLIB.ORG

CHOOSE DATABASES

☑ AFLOWLib ☑ Structure Properties ☐ Electronic Properties ☐ Thermoelectric Properties ☐ Scintillator Database ☑ Magnetic Properties ☐ Job Status

SEARCH AFLOWLIB (379,310 Compounds)
(188,768 Heusler Alloys; 173,324 Binary Alloys; 17,218 ICSD Compounds)

Element(s) Al & Mn & Ni — *Usage:* &(and), |(or), ~(not), ^(xor), m(metal) *e.g. ~Si and Al: having Al but not Si*
Species number 3
Material Type any type — Prototype Heusler (AlCu2Mn)
Lattice System any lattice system — Bravais Lattice any lattice (structure properties)
Space Group Number — Pearson Symbol (structure properties)
Minimum band gap = 0 eV — Maximum band gap = 17.506 eV (electronic properties)
Band Gap Type All types (electronic properties)
Minimum $\langle P_n \rangle / L$ = 0.00 μW/cmK²nm — Maximum $\langle P_n \rangle / L$ = 16025.65 μW/cmK²nm (thermoelectric properties)
Minimum $\langle P_p \rangle / L$ = 0.00 μW/cmK²nm — Maximum $\langle P_p \rangle / L$ = 34373.53 μW/cmK²nm (thermoelectric properties)
Minimum magnetic moment = 0.00 μ_B/atom — Maximum magnetic moment = 223.99 μ_B/atom (magnetic properties)
Minimum $\Delta S(E_F)$ = 0.00 — Maximum $\Delta S(E_F)$ = 1.00 (magnetic properties)
AFlow version from 299523 to 30427 — Calculated date from 2009-10-07 to 2012-07-31 (Job status)

(b)

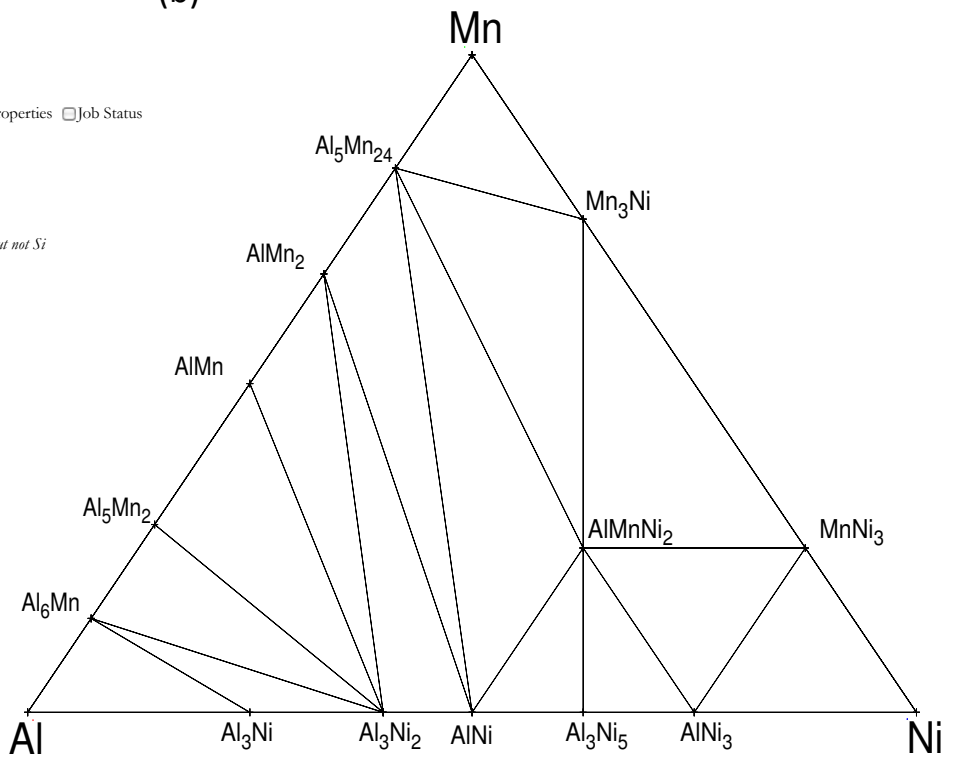

Curtarolo *et al.*, *"AFLOWLIB.ORG: a distributed materials properties repository from high-throughput ab initio calculations"*, Comp. Mat. Sci. **58**, 227-235 (2012).

$Al_1Ca_1O_5Ta_1$ (ICSD# 99001)

Real Space Lattices

Lattices:	a = 7.40Å b = 7.97Å c = 7.71Å α = 68.69° β = 90.00° γ = 90.00°
Volume:	423.76Å^3
Unit Cell Atom Number:	32
Space Group Number:	14
Pearson Symbol:	mP32
Lattice Primitive:	MCL Al1Ca1O5Ta1 #14.0 - (Al1Ca1O5Ta1_ICSD_99
Lattice Variation:	MCL
Crystal Family:	Monoclinic
Crystal System:	Monoclinic
Crystal Class:	Monoclinic-prismatic
Point Group (Hermann Mauguin):	2/m PGXTAL
Point Group (Schoenflies):	C_2h
Point Group Orbifold:	2*
Point Group Type:	centrosymmetric
Point Group Order:	4
Point Group Structure:	2 X Cyclic
Superlattice Primitive unit cell:	MCL
Superlattice Variation:	MCL
Pearson Symbol Superlattice:	mP32

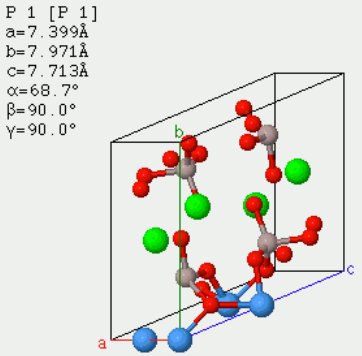

☑ Turn spin off

☐ Show atom labels

ball and stick

Density:	5.45 g/cm^3
Band Gap:	2.68 eV
Fit Band Gap:	4.53 eV
Band Gap Type:	Indirect
Electron Mass:	6.66 (m_0)
Hole Mass:	2.85 (m_0)

Reciprocal Space Lattices

Reciprocal Lattices:	a = 0.85Å b = 0.85Å c = 0.87Å α = 111.31° β = 90.00° γ = 90.00°
Volume:	0.59 Å^{-3}
Lattice Primitive:	MCL
Lattice Variation:	MCL

MCL path: Γ-Y-H-C-E-M_1-A-X-Γ-Z-D-M|Z-A|D-Y|X-H_1

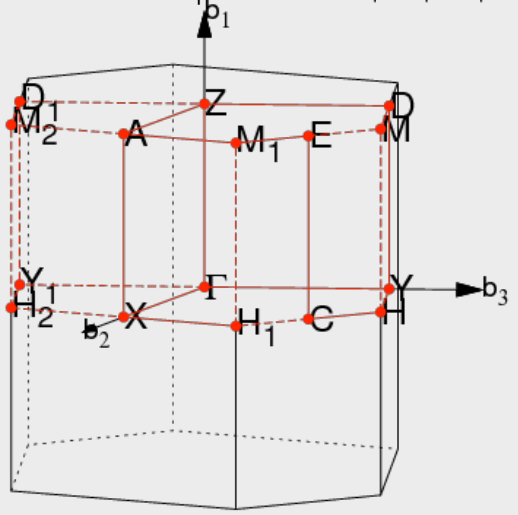

Electronic Properties

Band Structure

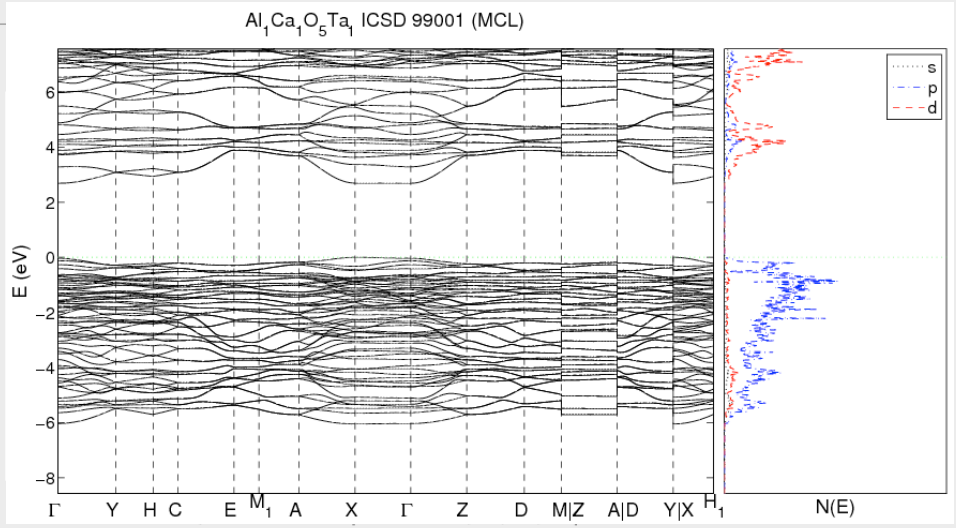

Comp. Mat. Sci. ***49***, 299-312 (2010)

Repository of quantum mechanics calculations

geometrical, structural data (lattice parameters, energies ☺)

thermoelectric data (power factors etc.)

▲Name [1]	ICSD Number [1]	Bravais Lattice	Number of Atoms	<P_n>/L (μW/cmK²nm) [4]	<P_{n1}>/L (μW/cmK²nm) [4]	<P_{n2}>/L (μW/cmK²nm) [4]	<P_{n3}>/L (μW/cmK²nm) [4]	<P_p>/L (μW/cmK²nm) [4]	<P_{p1}>/L (μW/cmK²nm) [4]	<P_{p2}>/L (μW/cmK²nm) [4]	<P_{p3}>/L (μW/cmK²nm) [4]	S_n (μV/K) [4]	S_p (μV/K) [4]
$F_3Fe_1K_1$	15424	CUB (Cubic)	5	0.15	0.15	0.15	0.15	2.17	2.17	2.17	2.17	-116.36	91.29
$F_3Fe_1Rb_1$	49586	CUB (Cubic)	5	0.24	0.24	0.24	0.24	1.50	1.48	1.51	1.51	-91.73	91.04
$Fe_1La_1O_3$	29118	CUB (Cubic)	5	0.31	0.31	0.31	0.31	2.00	2.00	2.00	2.00	-139.02	92.92
$Ag_2Fe_1S_4Sn_1$	42534	BCT (Tetragonal)	8	121 (I-42m)	tI16	4.77							

magnetic properties (if you want rare-earth-free magnets/spintronics)

scintillation properties/search

▲Name [1]	ICSD Number [1]	Bravais Lattice	Number of Atoms	Magnetic Moment (μB/atom) [5]	Spin Polarization (1/atom) [5]	Spin Decomposition (μB)
$Ag_1Fe_1O_2$	2786	HEX (Hexagonal)	8	1.25	0.00	{0.039,0.039,4.303,4.303,0.258,0.258,0.258,0.258}
$Ag_1Fe_1O_2$	31919	RHL (Rhombohedral)	4	1.25	0.00	{0.039,4.303,0.258,0.258}
$Ag_2Fe_1S_4Sn_1$	42534	BCT (Tetragonal)	8	0.50	0.00	{0.016,0.016,3.631,0.024,0.024,0.024,0.024,0.016}
F_2Fe_1	9166	TET (Tetragonal)	6	2.63 (I)	4.46	0.49	0.48	190.80	5.47	388.39	7.15	15.23	2.86700

Automatic Generation of Databases

Creating "aflow.in" input files:

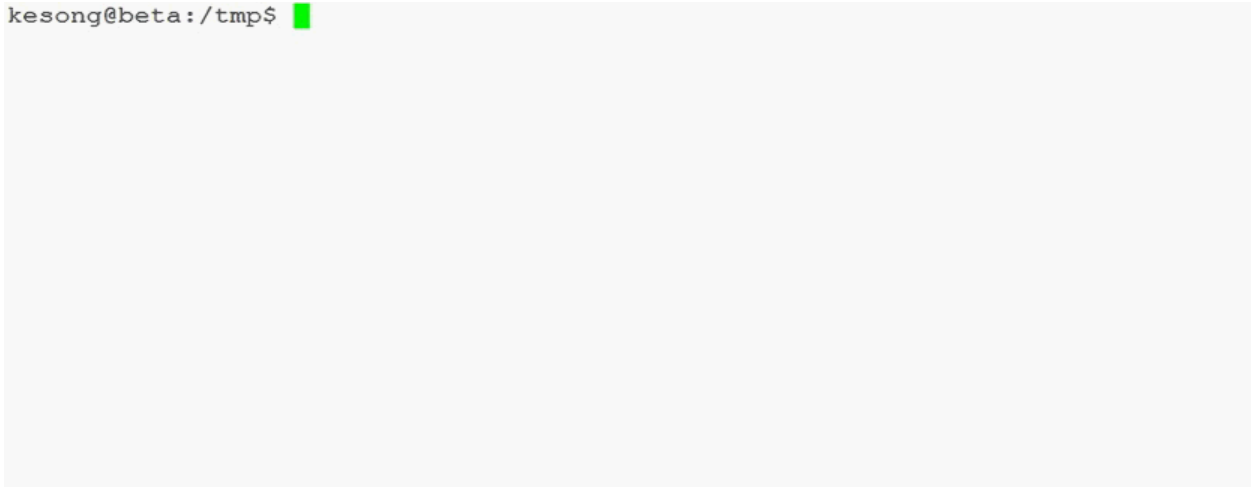

HT Computational Tools (AFLOW)

+

VASP

Materials Database (AFLOWLIB)

AFLOWLIB.ORG: a distributed materials properties repository from HT ab initio calculations, Comp. Mat. Sci. **58**, 227 (2012)

Automatic data/visualization analysis

Extract general materials properties: structural, electronic, magnetic properties…

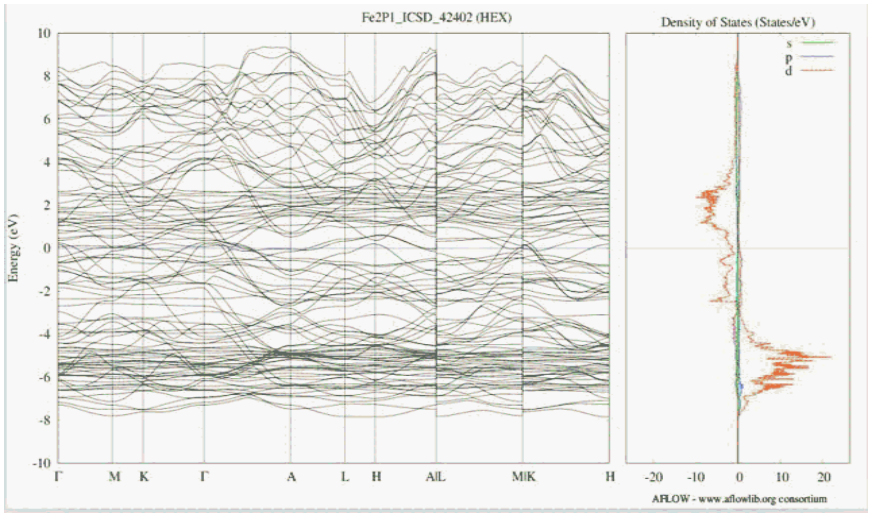

Develop new high-throughput programs based on the desired materials properties

AFLOW: an automatic framework for high-throughput materials discovery, Comp. Mat. Sci. **58**, 218-226 (2012)

Vibrational Free energy

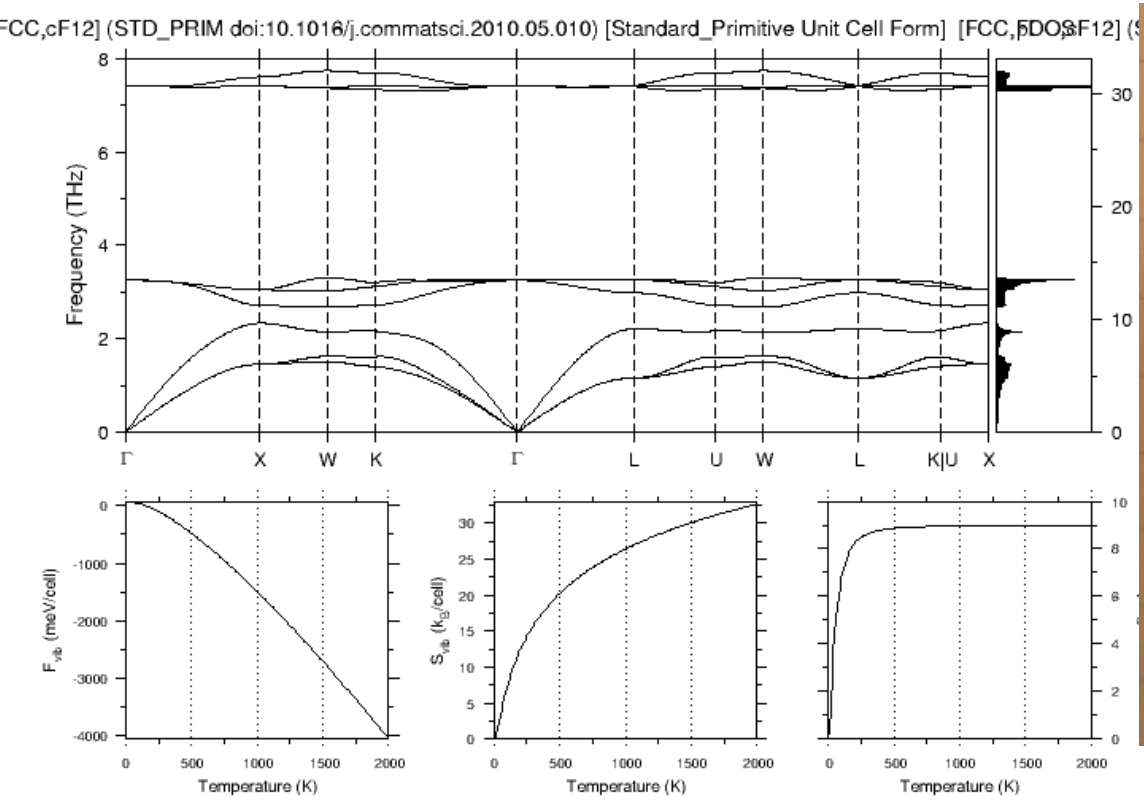

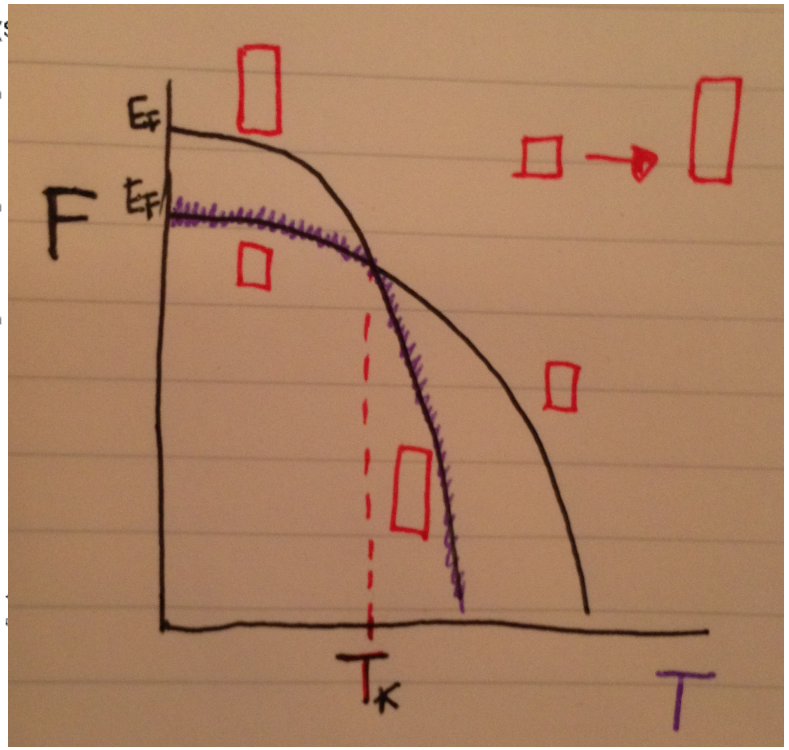

AFLOW: an automatic framework for high-throughput materials discovery, Comp. Mat. Sci. **58**, 218-226 (2012)

EXAMPLE: Topological Insulators

Table 1 | Examples of descriptors introduced in the literature. Nature Mater. **12**, 191 (2013)

Problem	Combination of materials properties (gene)	Descriptor
Structure stability: convex hull of an alloy system	Formation enthalpy (H_f) as a function of concentration (x) and the enthalpies (H) of A and B.	$H_f(x) = H(A_{1-x}B_x) - (1-x)H(A) - xH(B)$
Phase stability in off-lattice alloys PRL **91**, 135503 (2003)	Spectral decomposition of alloy vector-energies ($E_{n,p}$, n-rows = species, p-columns = configurations) with principal-component-analysis coefficients (α_i) and truncation error ($\epsilon(d)$) (ref. 3).	$E_{n,p} \simeq \alpha_1 E_{n,1} + \cdots + \alpha_{p-1} E_{n,p-1} + \epsilon(d)$
Nanosintered thermoelectrics PRX **1**, 021012 (2011)	Ratio of the average power factor ($<P>$) to the grain size (L) (ref. 15).	$\hat{\chi}_{\text{thermo}} \equiv \frac{<P>}{L}$
Topological insulators (epitaxial growth) Nature Mater. **11**, 614 (2012)	Variational ratio of spin–orbit distortion versus non-spin–orbit derivative strain (E_k^{SOC}, E_k^{noSOC}, spin/no spin–orbit bandgaps at k, a_0 lattice)[16].	$\hat{\chi}_{\text{TI}} \equiv - \frac{E_k^{SOC}(a_0)/a_0}{\delta E_k^{noSOC}(a)_0/\delta a_0\big\vert_{a_0}}$
Power conversion efficiency of a solar cell (spectroscopic limited maximum efficiency) PRL **108**, 068701 (2012)	Ratio of the maximum output power density (P_m) to the incident solar energy density (P_{in}) — a function (η) of the radiative electron–hole recombination current (f_r) and the photon absorptivity ($\alpha(E)$) — versus bandgap energy (E_g)[62].	$\eta(\alpha(E), f_r) = P_m/P_{in}; E_g$
Non-proportionality in scintillators IEEE Trans. Nucl. Sci. **56**, 2989 (2009)	Maximum mismatch between effective masses of electrons (m_e) and holes (m_h)[75].	$\hat{\chi}_{np} \equiv \max\left(\frac{m_e}{m_h}, \frac{m_h}{m_e}\right)$
Morphotropic phase boundary piezoelectrics PRB **84**, 014103 (2011)	Energy proximity between tetragonal, rhombohedra and rotational distortions (ΔE_p). Angular coordinate (α_{AB}) of the energy minimum in the A–B off-centerings energy map for ABO_3 systems[79].	$\Delta E_p \leq 0.5$ eV $\alpha_{AB} \approx 45°$

top. insul.

EXAMPLE: Topological Insulators

TI: insulator inside and conductor in the surface. The conducting state is protected by the symmetry of the system (inversion and time reversal).

Fu, Kane, Mele, PRL **98**, 106803 (2007).
Hasan, Kane, Rev. Mod. Phys. **82**, 3045 (2010).
Haldane, PRL **61**, 2015 (1988).
Nielssen, Ninomiya, Phys. Lett. 130B, 389 (1983).

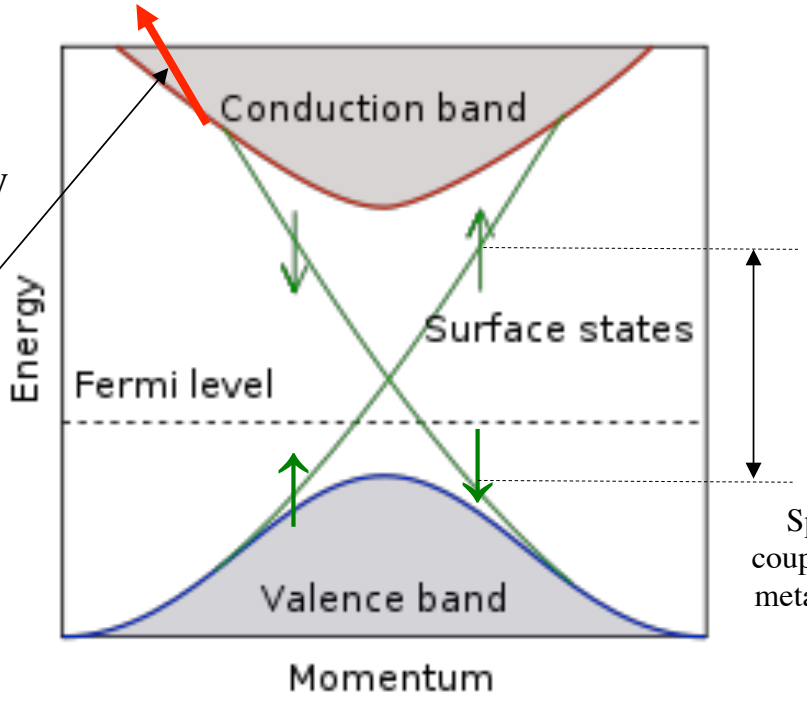

$$\hat{h}(\mathbf{k}) = \mathbf{h}(\mathbf{k}) / |\mathbf{h}(\mathbf{k})|$$

$$n = \frac{1}{4\pi} \int d^2\mathbf{k} (\partial_{k_x} \hat{h} \times \partial_{k_y} \hat{h}) \cdot \hat{h} \quad \text{(Berry Phase)}$$

number of times $\hat{h}(\mathbf{k})$ wraps around the unit sphere

each Dirac point contributes $\pm e^2/2h$ to σ_{xy}

Cones come in doubles (even).
Insulating state = cancellation => $\sigma_{xy}=0$
Quantum Hall State = summation => $\sigma_{xy} \neq 0$

EXAMPLES: going alloys and going surfaces

Surface *2D BZ*
Surface states

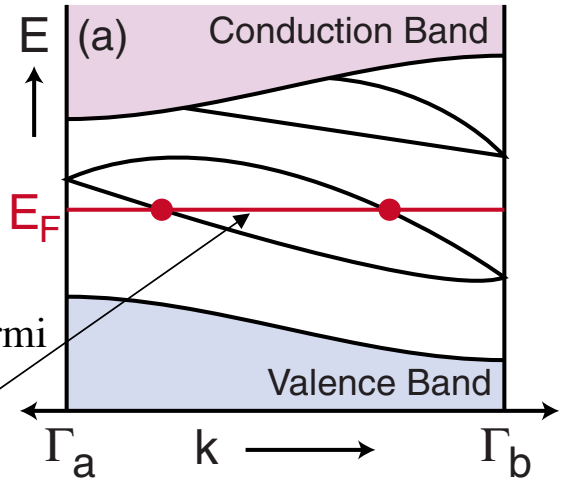

EVEN crossing 2D Fermi surface: destructable by troubles

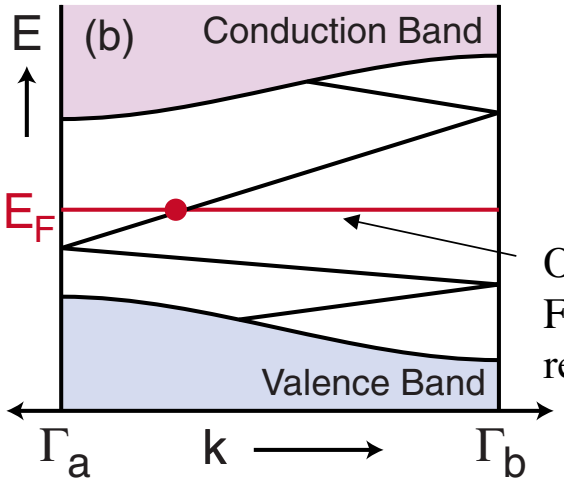

ODD crossing 2D Fermi surface: resistant

Time Reversal Invariant Momenta (TRIMs)

$$\Gamma_{i=(n_1 n_2 n_3)} = (n_1 \mathbf{b}_1 + n_2 \mathbf{b}_2 + n_3 \mathbf{b}_3)/2, \quad \text{with} \quad n_j = 0, \quad 1.$$

(a) **Bulk:** Roto-translational invariant (Noether's theorem)

$\rightarrow E^{SOC} < 0 \rightarrow E_p < E_s$

(c) **Surface**: TRIM points (eigenpoints solid-solution disorder operator)

(b) **Interface**: Roto-translational variant (Noether's theorem)

$\rightarrow E^{SOC} \sim 0 \rightarrow E_p > E_s$

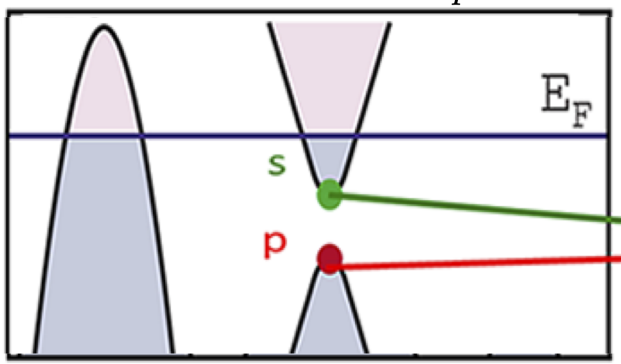

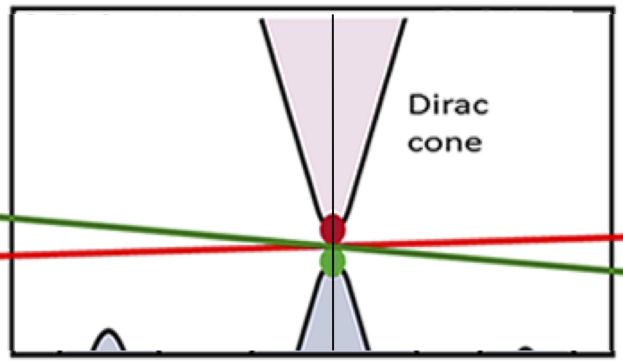

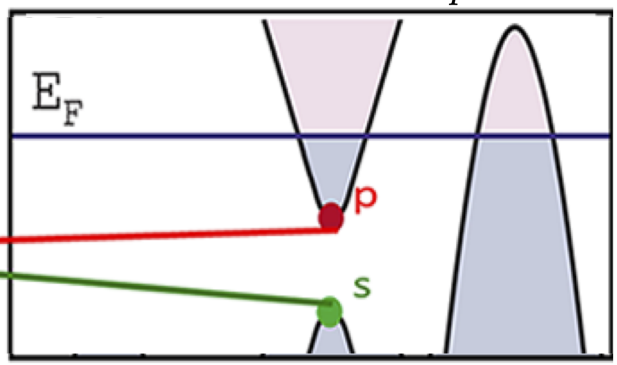

EXAMPLE: plain of action

- *Scan the aflowlib.org library*
- *Need of a **DESCRIPTOR (need to grow… epixially).***
- *search for combination of heavy metals (potential strong spin-orbit coupling)*
- *search for ideal band structures with appropriate gaps*
- *calculate band structure with LS (thousand of compounds)*
- *calculate the bands for surfaces to see localized conducting surface stares*
- *usually they contain Bi and/or Sb,Te, Pb.*

nature materials

ARTICLES

PUBLISHED ONLINE: XX MONTH XXXX | DOI: 10.1038/NMAT3332

A search model for topological insulators with high-throughput robustness descriptors

Kesong Yang[1], Wahyu Setyawan[2], Shidong Wang[1], Marco Buongiorno Nardelli[3,4] and Stefano Curtarolo[1,4,5]★

*Nature Materials,**11**(7), 614-619 (2012) DOI: 10.1038/nmat3332*

Let`s precess, epitaxially !

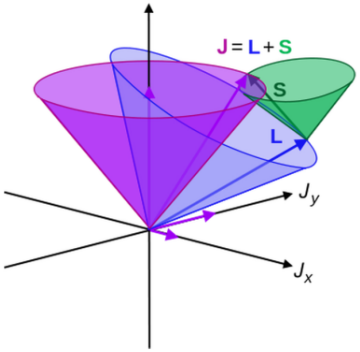

α) SPIN orbit calculations are expensive

β) LS due to electrons precessing near cores

γ) E^{soc}-E^{noSOC} ~ const

δ) simulated epitaxial strain with E^{noSOC}

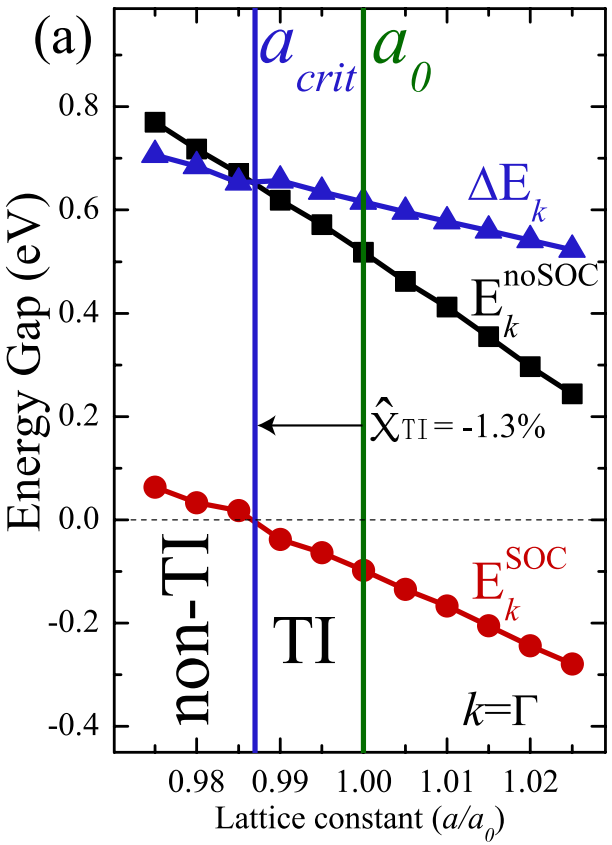

Bi_2Te_2S at $k = \Gamma$

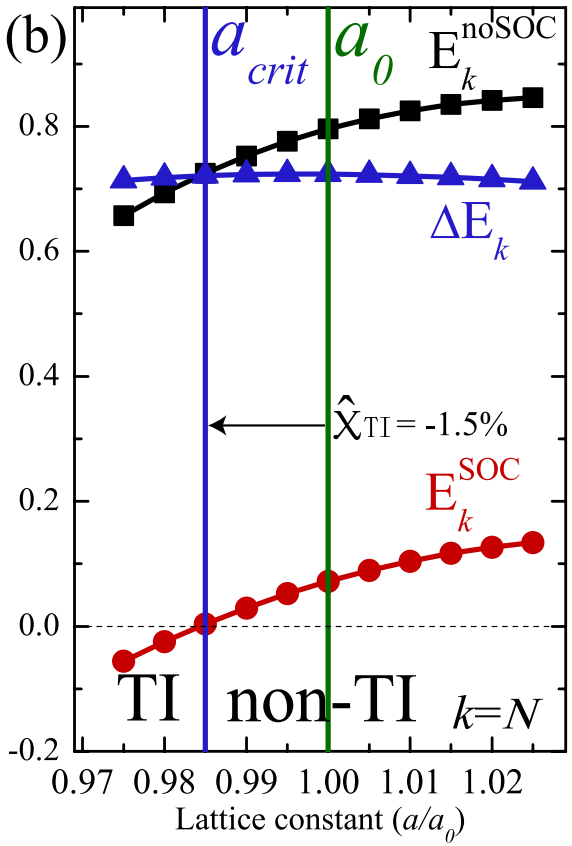

PbTe at $k = N$

covalent systems

ionic compounds

robustness descriptor varitional ("quasi-meaningful" quantity)

$$\hat{\chi}_{TI} \equiv -\frac{E_k^{SOC}(a_0)/a_0}{\delta E_k^{noSOC}(a)/\delta(a)\big|_{a_0}}$$

top. insul.

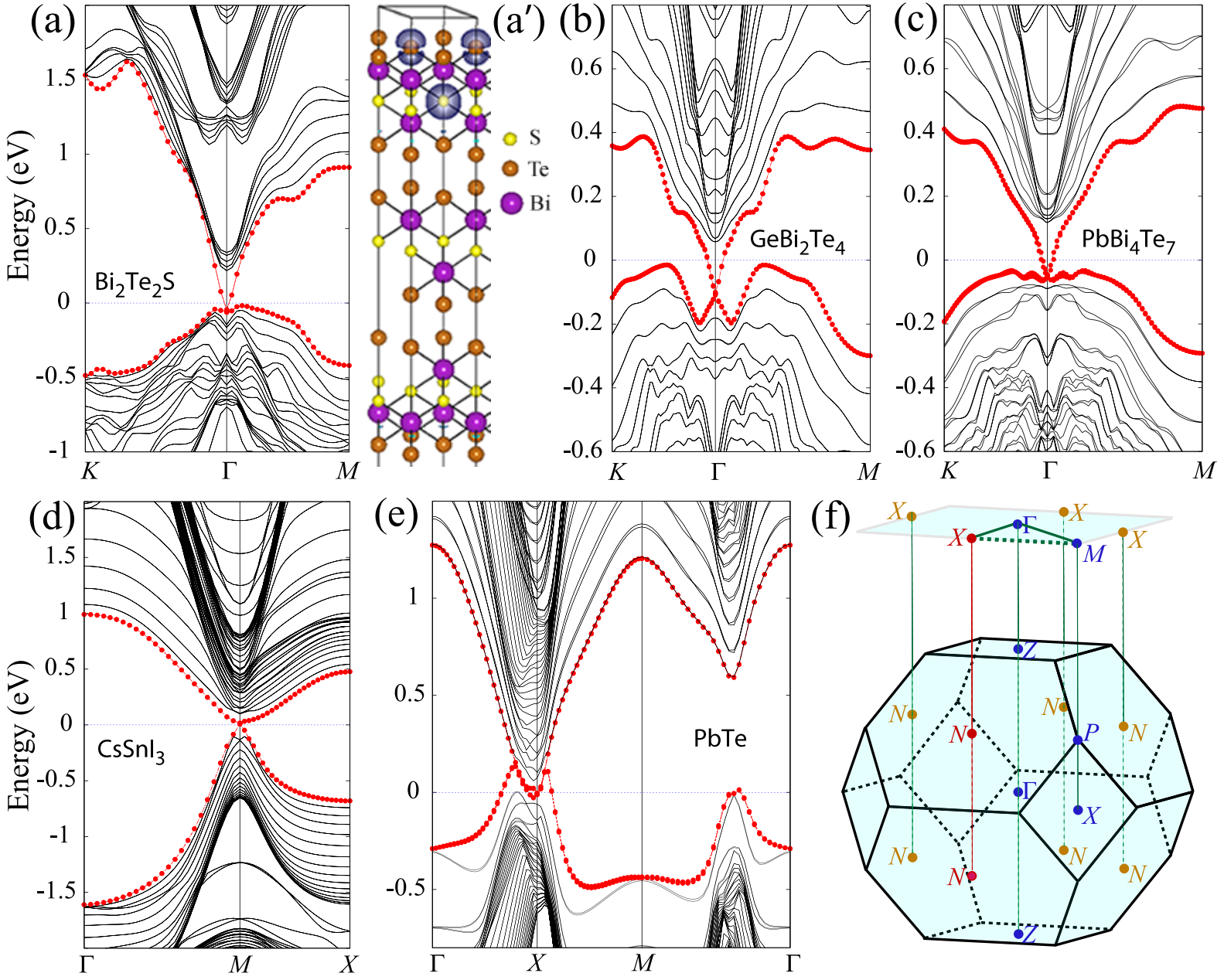
(a)
Energy (eV)
1.5
1
0.5
0
-0.5
-1
Bi_2Te_2S
K
Γ
M
(a′)
S
Te
Bi
(b)
0.6
0.4
0.2
0
-0.2
-0.4
-0.6
$GeBi_2Te_4$
K
Γ
M
(c)
0.6
0.4
0.2
0
-0.2
-0.4
-0.6
$PbBi_4Te_7$
K
Γ
M
(d)
Energy (eV)
1.5
1
0.5
0
-0.5
-1
-1.5
$CsSnI_3$
Γ
M
X
(e)
1
0.5
0
-0.5
PbTe
Γ
X
M
Γ
(f)
X
Γ
X
X
M
Z
N
N
N
P
N
Γ
X
N
N
N
N
Z

top. insul.

New compounds: tern. halides: $Cs\{Sn,Pb,Ge\}\{Cl,Br,I\}_3$

Table 1 | Properties of bulk and simulated epitaxial structures.

					Bulk												
							Simulated epitaxial growth (a optimized, c/a free)										
Compound	Space group	ICSD # ref. 31	Pearson symbol	Latt. ref. 39	Exp. a_0, c_0	DFT a_0, c_0	Pearson symbol	Latt. cleav.	a_{crit} (Å)	E_k^{SOC} 'ref'	Ref. lattice	E_g^{SOC} 'ref'	TRIM (mult.)	ΔE_k @ (a_0, c_0)	E_k^{SOC} @ (a_0, c_0)	$\hat{\chi}_{TI}$ (%)	
Sb_2Te_2S	$R\bar{3}m$	–	hR5	rhl_1	–	4.192	hR5	rhl_1	$1.006a_0$	−0.106	$1.019a_0$	0.106	Γ (1)	0.21	0.043	0.6	
						31.001		(0001)	$0.993c_0$		$0.975c_0$	(D)				PF	
Bi_2Te_2S	$R\bar{3}m$	617050	hR5	rhl_1	4.33	4.297	hR5	rhl_1	$0.987a_0$	−0.089	a_0	0.089	Γ (1)	0.62	−0.089	−1.3	
Fig. 2a					30.07	31.513		(0001)	$1.013c_0$		c_0	(D)				R	
$SnSb_2Te_4$	$R\bar{3}m$	30392	hR7	rhl_1	4.312	4.389	hR7	rhl_1	$0.999a_0$	−0.065	$1.011a_0$	0.065	Z(1)	0.22	0.013	−0.1	
					41.72	42.347		(0001)	$0.998c_0$		$0.984c_0$	(D)				PF	
$PbSb_2Te_4$	$R\bar{3}m$	250250	hR7	rhl_1	4.35	4.413	hR7	rhl_1	$0.988a_0$	−0.017	a_0	0.017	Z(1)	0.35	−0.017	−1.2	
					41.712	42.792		(0001)	$1.011c_0$		c_0	(D)				R	
$PbBi_4Se_7$	$P\bar{3}m1$	ref. 49	hP12	hex	4.25	4.216	hP12	hex	$1.018a_0$	−0.016	$1.023a_0$	0.016	A(1)	0.41	0.128	2.3	
					22.68	23.839		(0001)	$0.971c_0$		$0.966c_0$	(D)				PF	
$CsSnCl_3$	$Pm\bar{3}m$	28082	cP5	cub	5.504	5.618	tP5	tet	$0.951a_0$	−0.281	$0.936a_0$	0.111	A(1)	0.34	0.646	−4.9	
					5.504	5.618		(001)	$1.022c_0$		$1.209c_0$	(I)				HF	
$CsPbCl_3$	$Pm\bar{3}m$	29072	cP5	cub	5.605	5.733	tP5	tet	$0.914a_0$	−0.450	$0.890a_0$	0.354	A(1)	1.11	1.073	−8.6	
					5.605	5.733		(001)	$1.037c_0$		$1.050c_0$	(I)				HF	
$CsGeBr_3$	$Pm\bar{3}m$	80320	cP5	cub	5.36	5.603	tP5	tet	$0.955a_0$	−0.055	$0.952a_0$	0.026	A(1)	0.16	0.591	−4.5	
					5.36	5.603		(001)	$1.022c_0$		$1.023c_0$	(I)				HF	
$CsSnBr_3$	$Pm\bar{3}m$	4071	cP5	cub	5.795	5.884	tP5	tet	$0.972a_0$	−0.099	$0.965a_0$	0.099	A(1)	0.34	0.288	−2.8	
					5.795	5.884		(001)	$1.010c_0$		$1.013c_0$	(D)				PF	
$CsPbBr_3$	$Pm\bar{3}m$	29073	cP5	cub	5.874	5.993	tP5	tet	$0.934a_0$	−0.120	$0.926a_0$	0.120	A(1)	1.11	0.641	−6.6	
					5.874	5.993		(001)	$1.024c_0$		$1.027c_0$	(D)				HF	
$CsSnI_3$	$Pm\bar{3}m$	69997	cP5	cub	6.219	6.272	tP5	tet	$0.993a_0$	−0.335	$0.960a_0$	0.169	A(1)	0.39	0.070	−0.7	
Fig. 2d					6.219	6.272		(001)	$1.002c_0$		$1.013c_0$	(I)				PF	
SnTe	$Fm\bar{3}m$	52489	cF8	fcc	4.471	4.528	tI4	bct_2	$1.027a_0$	−0.058	$1.010a_0$	0.058	N (4)	0.15	−0.107	2.7	
					6.323	6.404		(001)	$0.998c_0$		$0.999c_0$	(D)				VR	

Properties of bulk structure: compound (∗ indicates experimental validation), space group, ICSD number[31], Pearson symbol, Bravais lattice[39], experimental and DFT equilibrium lattices a, c in (Å). Properties under the simulated epitaxial growth condition: Pearson symbol, Bravais lattice with conventional cleavage Miller indices, critical value for band inversion (a_{crit}), SOC band energy difference ($E_k^{SOC}(ref.)$) at the TRIM with the reference lattice, reference lattice, SOC band-gap at the reference lattice (direct/indirect) ($E_g^{SOC}(ref.)$), TRIMs having band inversion with multiplicity[39], SOC energy-gap discrepancy (ΔE_k) at the *ab initio* equilibrium lattice, SOC band energy difference ($E_k^{SOC}(a_0)$) at the TRIM with the *ab initio* equilibrium lattice, HT-descriptor ($\hat{\chi}_{TI}$). The labels below $\hat{\chi}_{TI}$ indicate: F(fragile), R(robust), VR(very robust), PF(potentially feasible), and HF(hardly feasible) (structural and electronic data is available by following the links listed in the Supplementary Information Extended Table).

novel ternary halides

if $E_k^{SOC}(a_0) \leq 0$, **robustness**:
$|\hat{\chi}_{TI}| \leq 1\% \Rightarrow$ fragile,
$1\% < |\hat{\chi}_{TI}| \leq 2\% \Rightarrow$ robust,
$2\% < |\hat{\chi}_{TI}| \Rightarrow$ very-robust.

if $E_k^{SOC}(a_0) > 0$, **feasibility**:
$|\hat{\chi}_{TI}| \leq 3\% \Rightarrow$ potentially-feasible,
$3\% < |\hat{\chi}_{TI}| \Rightarrow$ hardly-feasible.

top. insul.

EXAMPLE: Topological Insulators

Projects on surfaces by aligning semicones and checking thermodynamics of planes

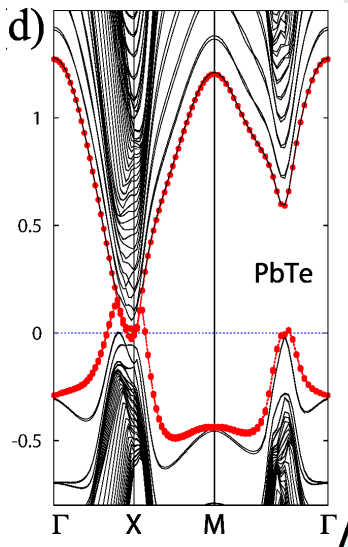

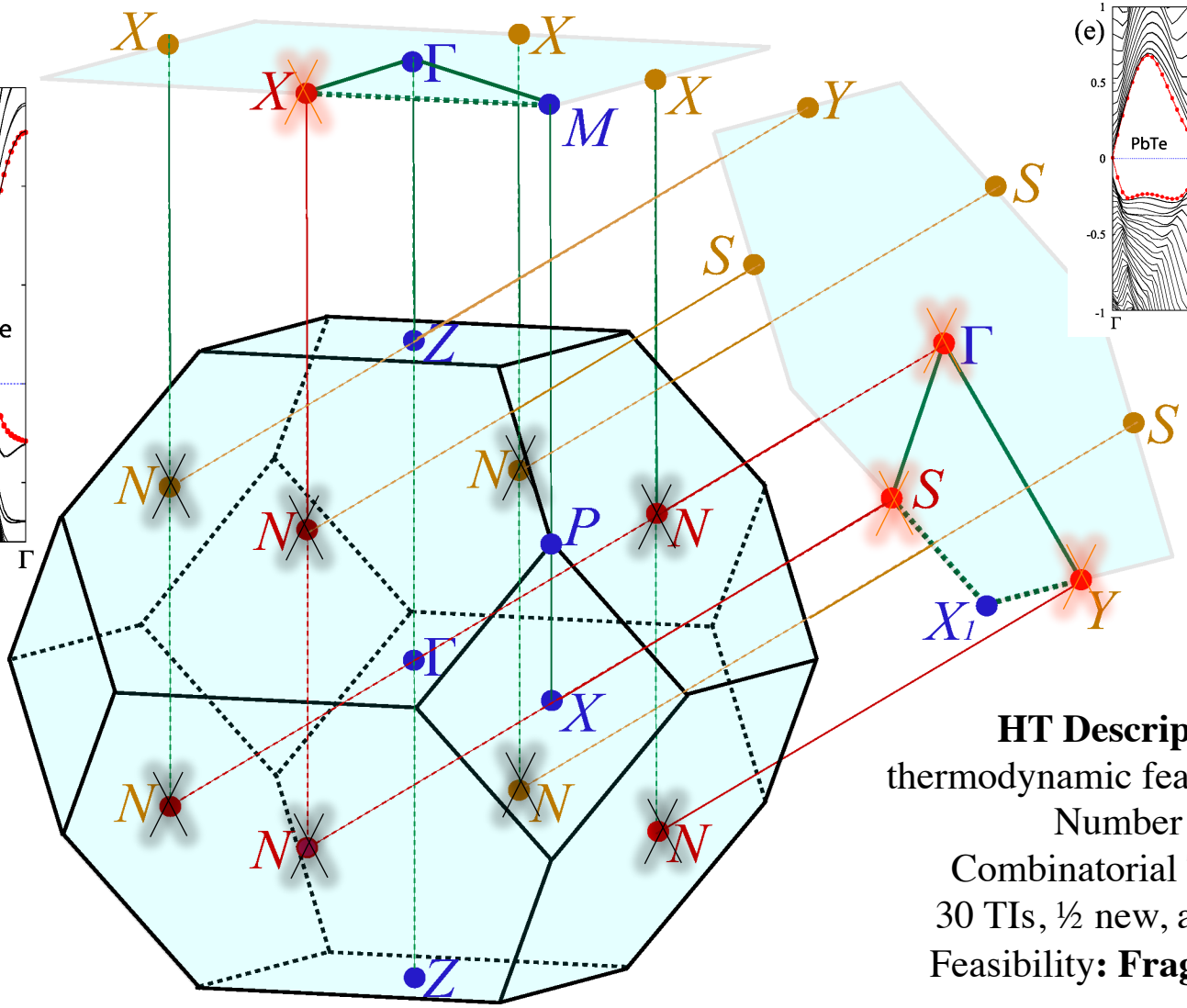

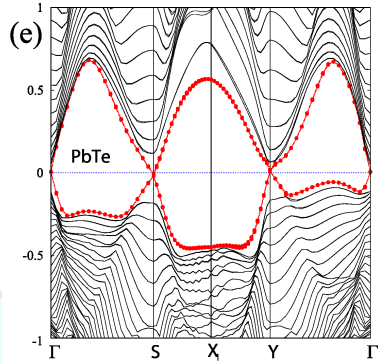

HT Descriptor based search
thermodynamic feasibility of surface
Number of cones "nailed"
Combinatorial TRIMs directions
30 TIs, ½ new, a few unguessable
Feasibility**: Fragility/Robustness**

Yang, Setyawan, Buongiorno Nardelli, **Curtarolo**: *High-Throughput Descriptor for Novel Topological Insulators, Nature Materials,**11**(7), 614-619 (2012) DOI: 10.1038/nmat3332*

EXAMPLE: Thermoelectrics

without the constant relaxation time approximation

Table 1 | Examples of descriptors introduced in the literature. Nature Mater. **12**, 191 (2013)

Problem	Combination of materials properties (gene)	Descriptor
Structure stability: convex hull of an alloy system	Formation enthalpy (H_f) as a function of concentration (x) and the enthalpies (H) of A and B.	$H_f(x) = H(A_{1-x}B_x) - (1-x)H(A) - xH(B)$
Phase stability in off-lattice alloys PRL **91**, 135503 (2003)	Spectral decomposition of alloy vector-energies ($E_{n,p}$, n-rows = species, p-columns = configurations) with principal-component-analysis coefficients (α_i) and truncation error ($\epsilon(d)$) (ref. 3).	$E_{n,p} \simeq \alpha_1 E_{n,1} + \cdots + \alpha_{p-1} E_{n,p-1} + \epsilon(d)$
Nanosintered thermoelectrics PRX **1**, 021012 (2011)	Ratio of the average power factor (<P>) to the grain size (L) (ref. 15).	$\hat{\chi}_{\text{thermo}} \equiv \frac{<P>}{L}$
Topological insulators (epitaxial growth) Nature Mater. **11**, 614 (2012)	Variational ratio of spin–orbit distortion versus non-spin–orbit derivative strain (E_k^{SOC}, E_k^{noSOC}, spin/no spin–orbit bandgaps at k, a_0 lattice)[16].	$\hat{\chi}_{TI} \equiv - \frac{E_k^{SOC}(a_0)/a_0}{\delta E_k^{noSOC}(a)_0/\delta a_0\big\vert_{a_0}}$
Power conversion efficiency of a solar cell (spectroscopic limited maximum efficiency) PRL **108**, 068701 (2012)	Ratio of the maximum output power density (P_m) to the incident solar energy density (P_{in}) — a function (η) of the radiative electron–hole recombination current (f_r) and the photon absorptivity ($\alpha(E)$) — versus bandgap energy (E_g)[62].	$\eta(\alpha(E), f_r) = P_m/P_{in}; E_g$
Non-proportionality in scintillators IEEE Trans. Nucl. Sci. **56**, 2989 (2009)	Maximum mismatch between effective masses of electrons (m_e) and holes (m_h)[79].	$\hat{\chi}_{np} \equiv \max\left(\frac{m_e}{m_h}, \frac{m_h}{m_e}\right)$
Morphotropic phase boundary piezoelectrics PRB **84**, 014103 (2011)	Energy proximity between tetragonal, rhombohedra and rotational distortions (ΔE_p). Angular coordinate (α_{AB}) of the energy minimum in the A–B off-centerings energy map for ABO_3 systems[79].	$\Delta E_p \leq 0.5$ eV $\alpha_{AB} \approx 45°$

EXAMPLE: Thermoelectricity

Thermoelectrics: convert flow of electronic entropy in electronic current

$$ZT = \frac{\sigma S^2 T}{\kappa}$$

$$P = \sigma S^2$$

$$ZT > 1 \Rightarrow S > 156\mu\mathrm{V/K}$$

from Wiedemann-Franz law (room T)

constant must increase less than k

$$ZT = \frac{\sigma S^2 T}{\kappa}$$

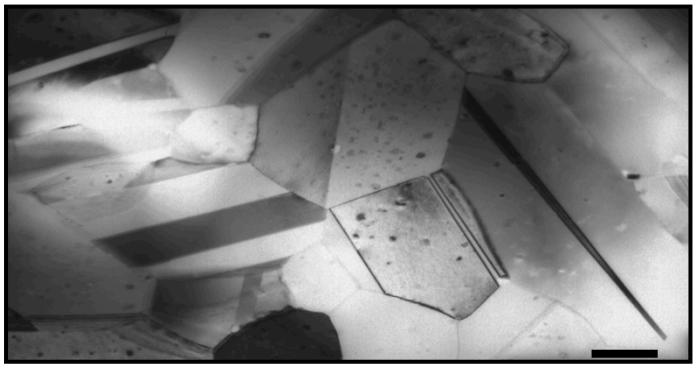

sintering
polycrystalline

Bi_2Te_3

must decrease

Courtesy: G. Bernard-Granger, LITEN, CEA-Grenoble.

EXAMPLE: Thermoelectricity

$$ZT = \frac{\sigma S^2 T}{\kappa} \qquad P = \sigma S^2$$

Sintered compounds have diffusive scattering for carriers (similar diffusive model of phonon transport [1])

Then mean free path is of the order of the grain: $\lambda \simeq L$ *(so we can play with L)*

From the **C**onstant **R**elaxation **T**ime **A**pproximation **(CRTA)** to **C**onstant **M**ean **F**ree **P**ath **A**pproximation **(CMFPA)** [2,3]

[1] PRB **67**, 054302 (2003), JAP **93**, 793 (2003), RMP **61**, 605 (1989), PRB **48**, 16373 (1993)
[2] JAP **108**, 124306 (2010)
[3] PRX **1**, 021012 (2011)

Constant Mean Free Path Approximation

PRX **1**, 021012 (2011)

$$ZT = \frac{\sigma S^2 T}{\kappa} \qquad P = \sigma S^2$$

$$\text{for materials usually: } \lambda_e^{\text{bulk}} < \lambda_{ph}^{\text{bulk}}$$

THREE SCENARIOS versus L

1. BIG GRAINS

$$\lambda_e^{\text{bulk}} < \lambda_{ph}^{\text{bulk}} < L \;\Rightarrow \{\sigma, \kappa\} \text{ need } \tau \text{ \& phons} \Rightarrow ZT$$

2. MEDIUM GRAINS

$$\lambda_e^{\text{bulk}} < L < \lambda_{ph}^{\text{bulk}} \;\Rightarrow \kappa \propto L \;\Rightarrow ZT \propto 1/L$$

3. TINY GRAINS

$$L < \lambda_e^{\text{bulk}} \;\Rightarrow \sigma, \kappa \propto L \;\Rightarrow ZT \sim const \;\Rightarrow P \propto L$$

Small grain size (SGS) limit

Constant Mean Free Path Approximation

PRX **1**, 021012 (2011)

$$ZT = \frac{\sigma S^2 T}{\kappa} \qquad P = \sigma S^2$$

for materials usually: $\lambda_e^{\text{bulk}} < \lambda_{ph}^{\text{bulk}}$

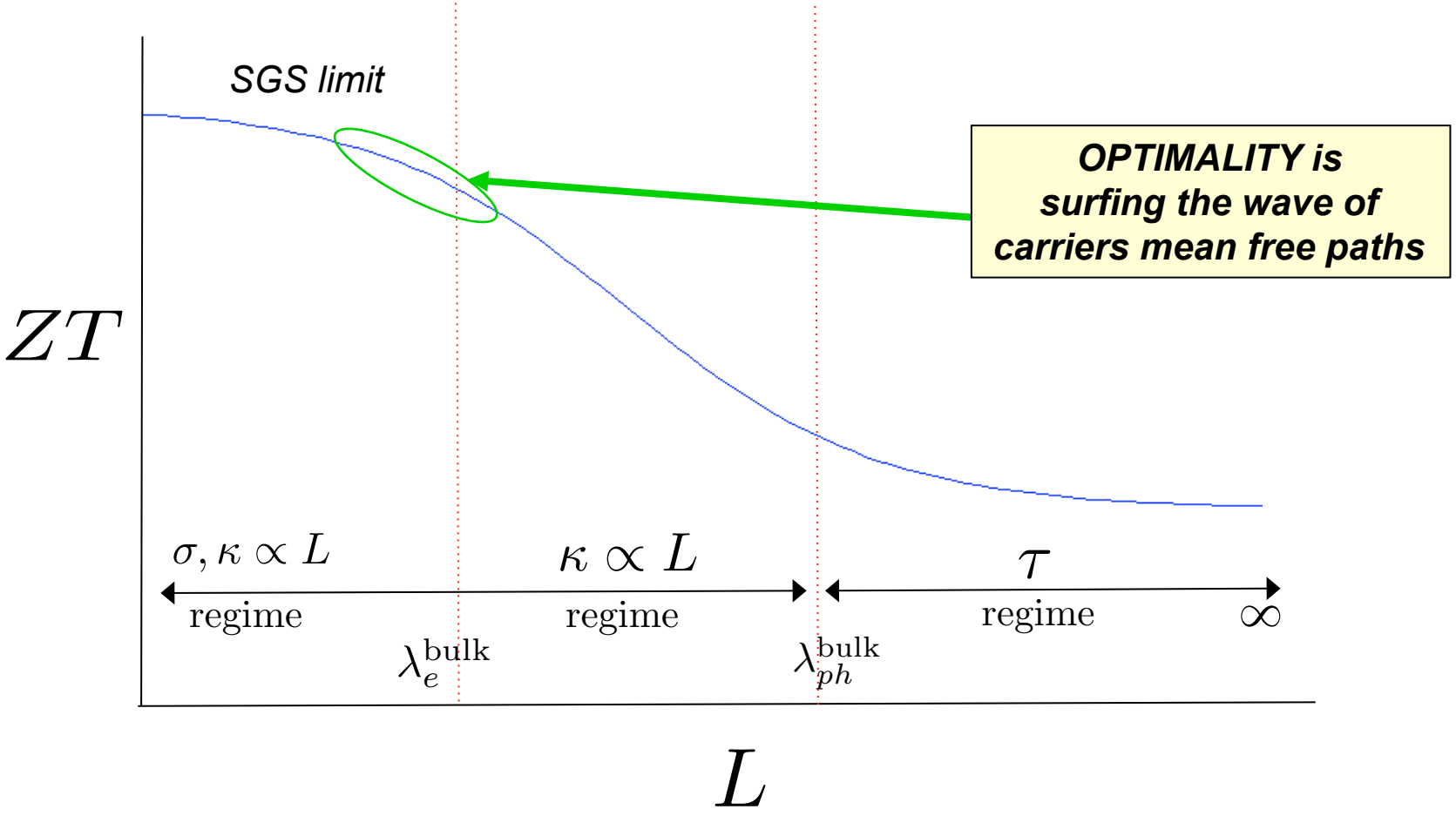

PRX **1**, 021012 (2011)

Calculation of the power factor, $S^2\sigma/L$ for ~13,000 compounds

Boltzmann transport equation solved inside AFLOW

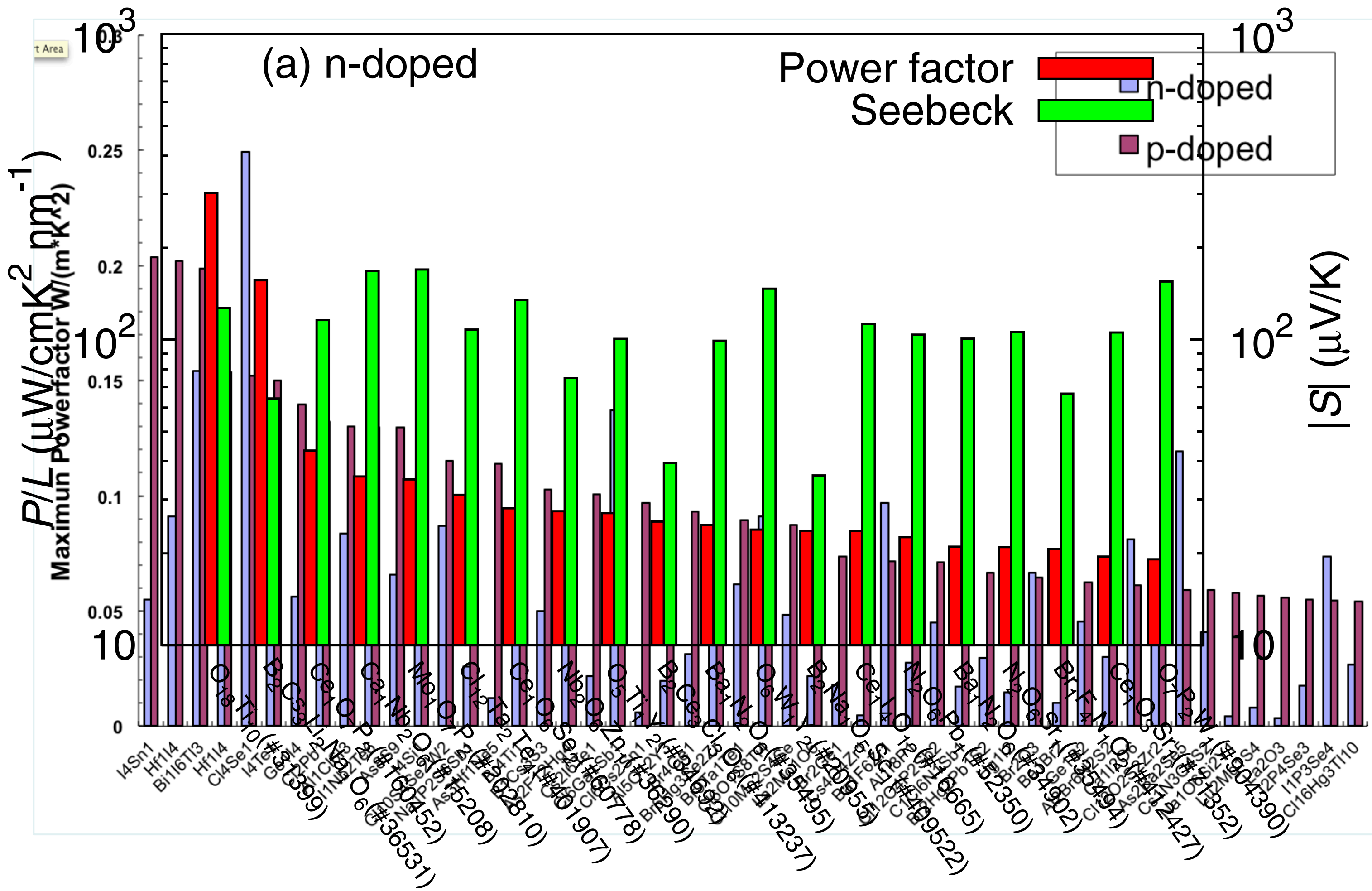

power factor

For sintered, depends on directions, project on principal axes

$X_{thermo}=<P>/L$

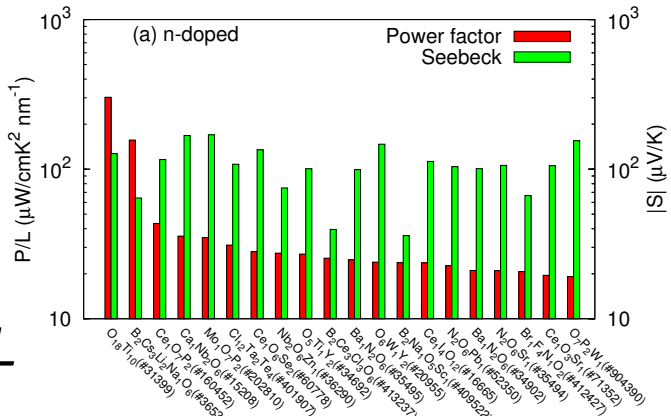

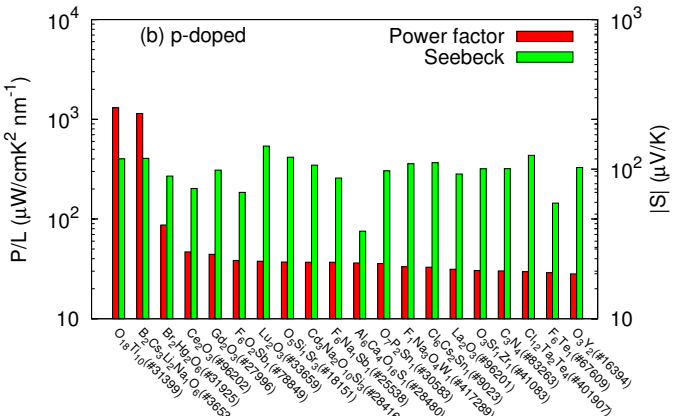

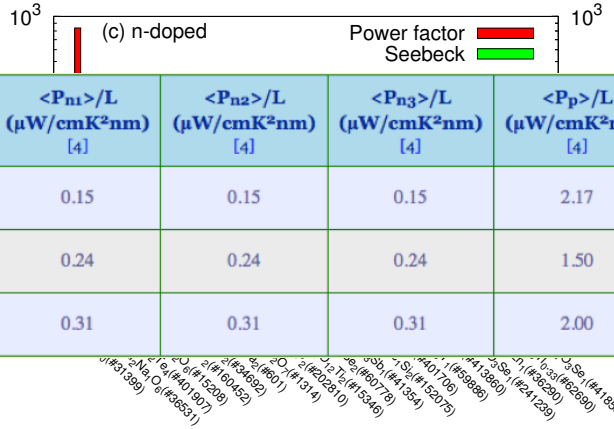

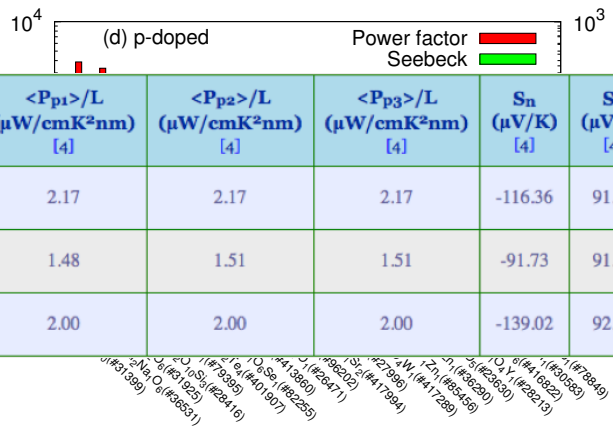

▲Name [1]	ICSD Number [1]	Bravais Lattice	Number of Atoms	<Pn>/L (μW/cmK²nm) [4]	<Pn1>/L (μW/cmK²nm) [4]	<Pn2>/L (μW/cmK²nm) [4]	<Pn3>/L (μW/cmK²nm) [4]	<Pp>/L (μW/cmK²nm) [4]	<Pp1>/L (μW/cmK²nm) [4]	<Pp2>/L (μW/cmK²nm) [4]	<Pp3>/L (μW/cmK²nm) [4]	Sn (μV/K) [4]	Sp (μV/K) [4]
$F_3Fe_1K_1$	15424	CUB (Cubic)	5	0.15	0.15	0.15	0.15	2.17	2.17	2.17	2.17	-116.36	91.29
$F_3Fe_1Rb_1$	49586	CUB (Cubic)	5	0.24	0.24	0.24	0.24	1.50	1.48	1.51	1.51	-91.73	91.04
$Fe_1La_1O_3$	29118	CUB (Cubic)	5	0.31	0.31	0.31	0.31	2.00	2.00	2.00	2.00	-139.02	92.92

max P_i/L

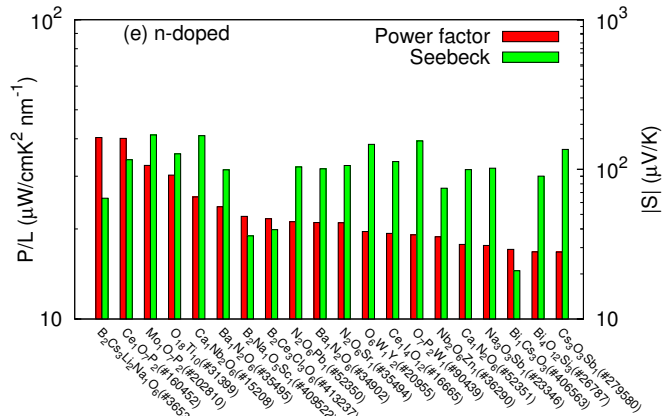

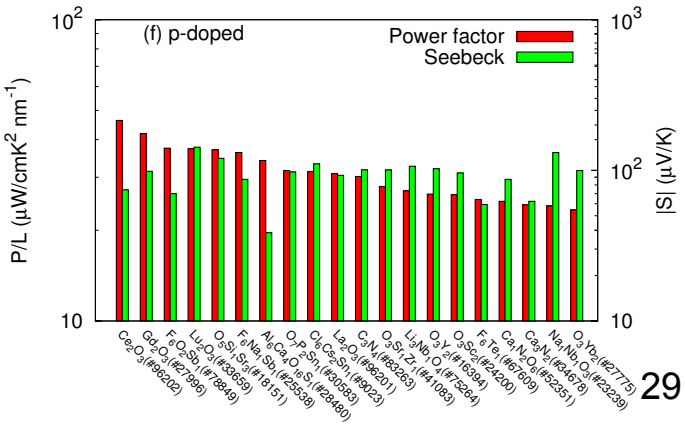

PRX **1**, 021012 (2011)

EXAMPLE 2: thermoelectricity: correlations

TABLE II. Calculated Pearson correlations between the normalized power factor and other properties: band gap (E_g), carriers' effective mass (m_e, m_h), and ratios between the maximum and minimum effective masses. Power factor is positively correlated to most of these properties.

Pearson correlations	E_g	m_e	m_h	m_e^{max}/m_e^{min}	m_h^{max}/m_h^{min}
Median P/L (μW/cmK^2)					
$\log(P_n/L)$	0.25	0.28		0.10	
$\log(P_p/L)$	0.40		0.07		0.00

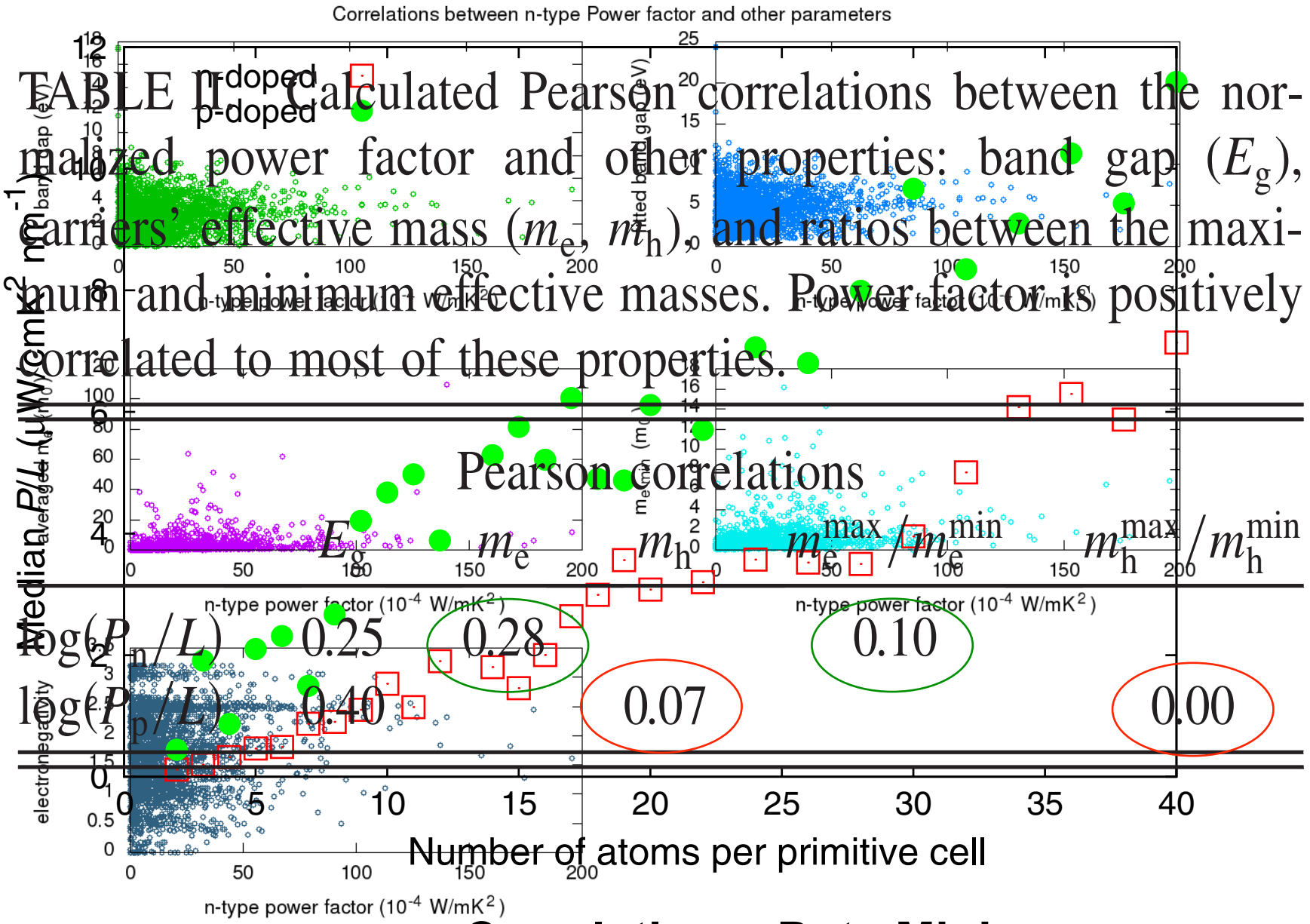

Correlations -Data Mining

PRX **1**, 021012 (2011)

EXAMPLE Scintillator Materials

Table 1 | Examples of descriptors introduced in the literature. Nature Mater. **12**, 191 (2013)

Problem	Combination of materials properties (gene)	Descriptor
Structure stability: convex hull of an alloy system	Formation enthalpy (H_f) as a function of concentration (x) and the enthalpies (H) of A and B.	$H_f(x) = H(A_{1-x}B_x) - (1-x)H(A) - xH(B)$
Phase stability in off-lattice alloys PRL **91**, 135503 (2003)	Spectral decomposition of alloy vector-energies ($E_{n,p}$, n-rows = species, p-columns = configurations) with principal-component-analysis coefficients (α_i) and truncation error ($\epsilon(d)$) (ref. 3).	$E_{n,p} \simeq \alpha_1 E_{n,1} + \cdots + \alpha_{p-1} E_{n,p-1} + \epsilon(d)$
Nanosintered thermoelectrics PRX **1**, 021012 (2011)	Ratio of the average power factor (<P>) to the grain size (L) (ref. 15).	$\hat{\chi}_{\text{thermo}} \equiv \frac{<P>}{L}$
Topological insulators (epitaxial growth) Nature Mater. **11**, 614 (2012)	Variational ratio of spin–orbit distortion versus non-spin–orbit derivative strain (E_k^{SOC}, E_k^{noSOC}, spin/no spin–orbit bandgaps at k, a_0 lattice)[16].	$\hat{\chi}_{TI} \equiv - \frac{E_k^{SOC}(a_0)/a_0}{\delta E_k^{noSOC}(a)_0/\delta a_0\big\vert_{a_0}}$
Power conversion efficiency of a solar cell (spectroscopic limited maximum efficiency) PRL **108**, 068701 (2012)	Ratio of the maximum output power density (P_m) to the incident solar energy density (P_{in}) — a function (η) of the radiative electron–hole recombination current (f_r) and the photon absorptivity ($\alpha(E)$) — versus bandgap energy (E_g)[62].	$\eta(\alpha(E), f_r) = P_m/P_{in}; E_g$
Non-proportionality in scintillators IEEE Trans. Nucl. Sci. **56**, 2989 (2009)	Maximum mismatch between effective masses of electrons (m_e) and holes (m_h)[75].	$\hat{\chi}_{np} \equiv \max\left(\frac{m_e}{m_h}, \frac{m_h}{m_e}\right)$
Morphotropic phase boundary piezoelectrics PRB **84**, 014103 (2011)	Energy proximity between tetragonal, rhombohedra and rotational distortion (ΔE_p). Angular coordinate (α_{AB}) of the energy minimum in the A–B off-centerings energy map for ABO_3 systems[79].	$\Delta E_p \leq 0.5$ eV $\alpha_{AB} \approx 45°$

Introduction: Nonproportionality

Previous studies revealed variations in nonproportionality for compounds with:

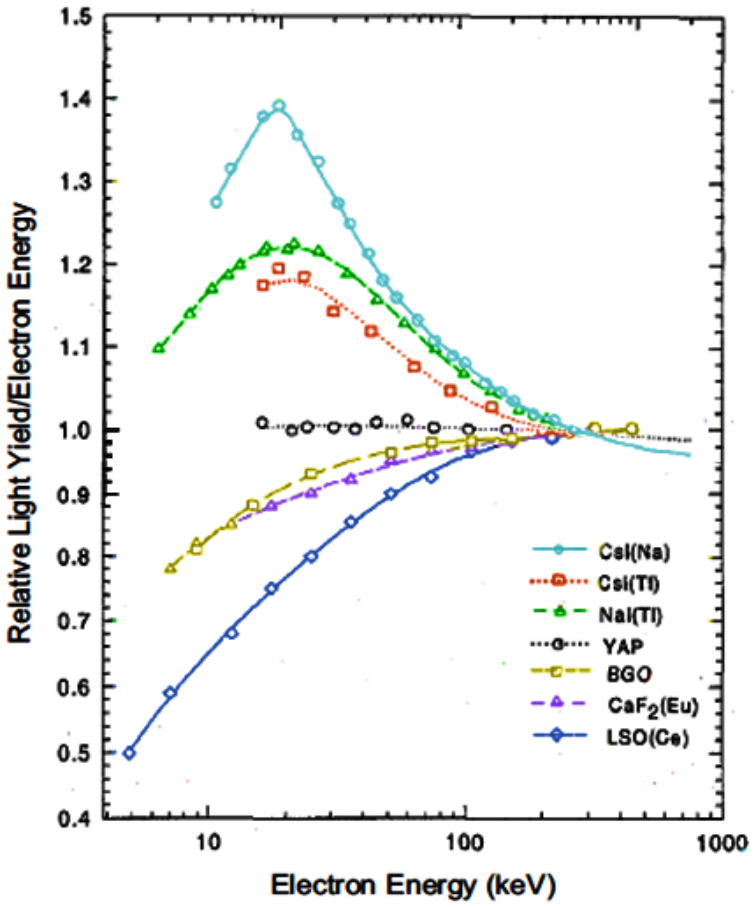

the same crystal-structure

Ce: $YAlO_3$ vs. Ce:$LuAlO_3$

cation substitutions

Ce: $(Gd_{1-x}Lu_x)_2SiO_5$

dopants

NaI vs Tl:NaI

crystal quality

defects and inhomogeneities

cation valence in multi-cation compounds

isovalent cations (ex. Ce:$Y^{3+}Al^{3+}O_3$) have better linearity than aliovalent cations (Ce:$Y^{3+}{}_2Si^{4+}O_5$)

temperature

Modeling: Nonproportionality & Band structure

Small Nonproportionality

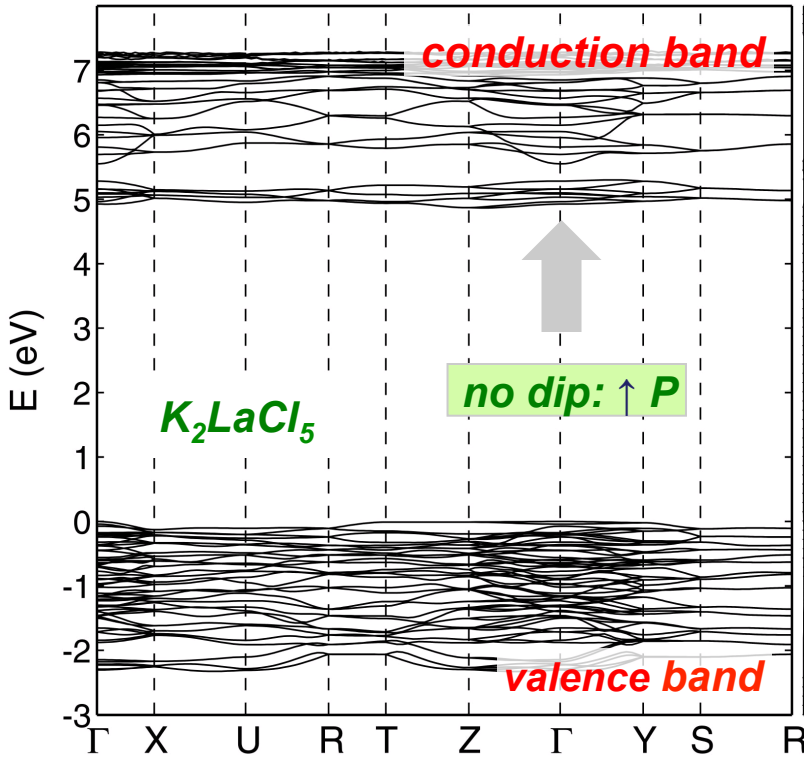

Large Nonproportionality

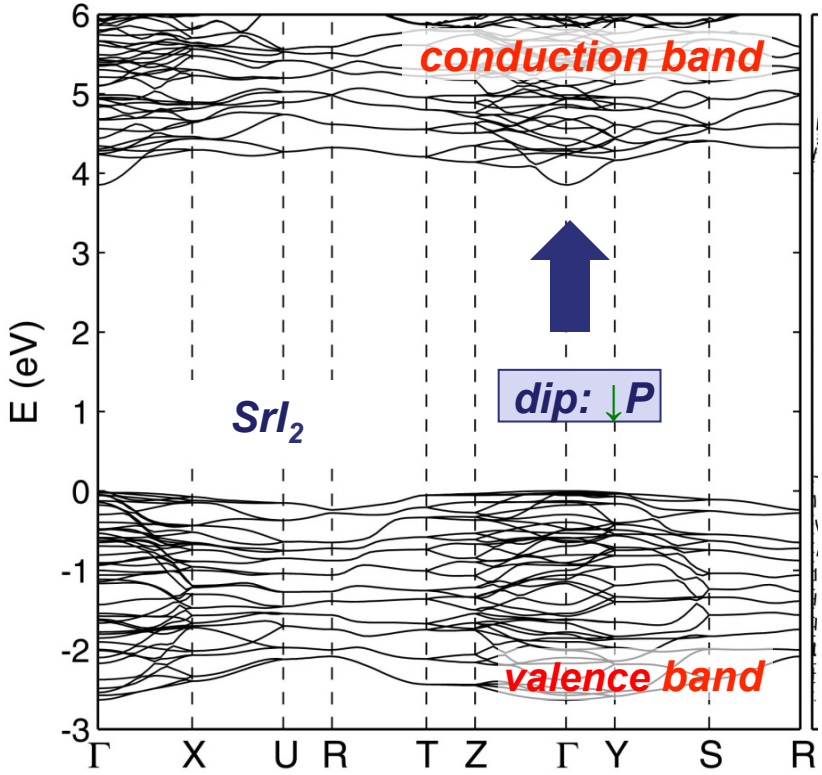

Presence of dip: ↓ m_e → P ↓

EXAMPLE: Modeling: NP vs. Effective ratio

$$NP_{10/662} = \frac{LY_{10keV}}{LY_{662keV}}$$

versus

$$m_r = max\left(\frac{m_e^\star}{m_h^\star}, \frac{m_h^\star}{m_e^\star}\right)$$

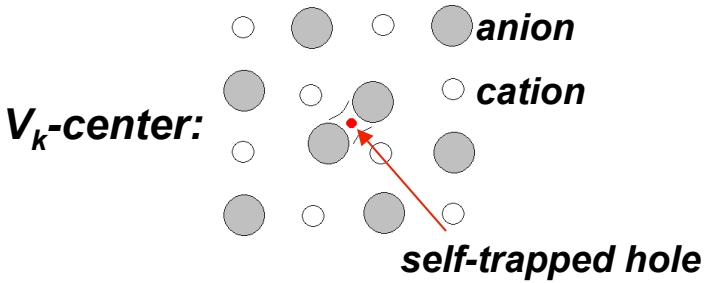

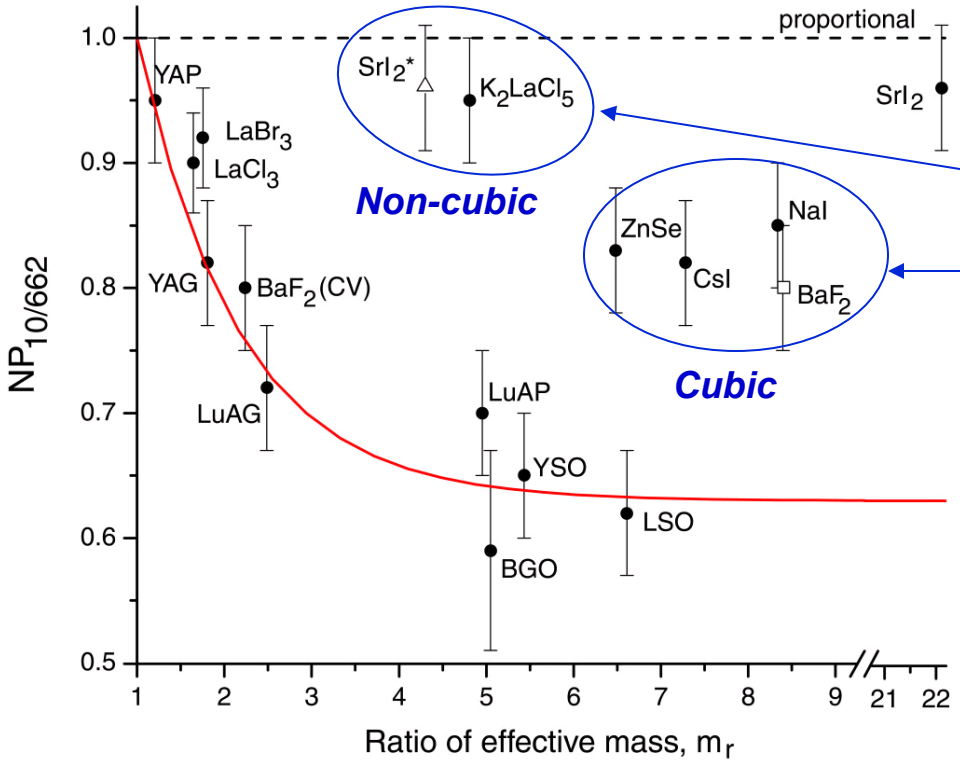

Free carriers in V_k compounds

- *Cubic (P ↓), ↓non-cubic (P ↑)*
- *V_k-centers act as additional traps.*
- *Effective trapping in isotropic media → P ↓*

Free carriers in non-V_k compounds

- *P ↑as m_r → 1*
- *Spatial distribution of free e/h depends on mass ratio.*
- *When free e/h are near luminescent centers, loss decreases → P ↑*

m_r ratios are pressure dependent

IEEE Trans. Nucl. Sci. ***56****, 2989 (2009).*

cub: *$Bi_4Ge_3O_{12}$(BGO), $Y_3Al_5O_{12}$(YAG), $Lu_3Al_5O_{12}$(LuAG), BaF_2, ZnSe, CsI, NaI, $BaHfO_3$,$SrHfO_3$, $LiBaF_3$.*
hex*: $LaBr_3$, $LaCl_3$* ***ort****: SrI_2, $YAlO_3$(YAP), $LuAlO_3$(LuAP), K_2LaCl_5(KLC)* ***mcl****: Y_2SiO_5(YSO), Lu_2SiO_5(LSO)*

Host material selection

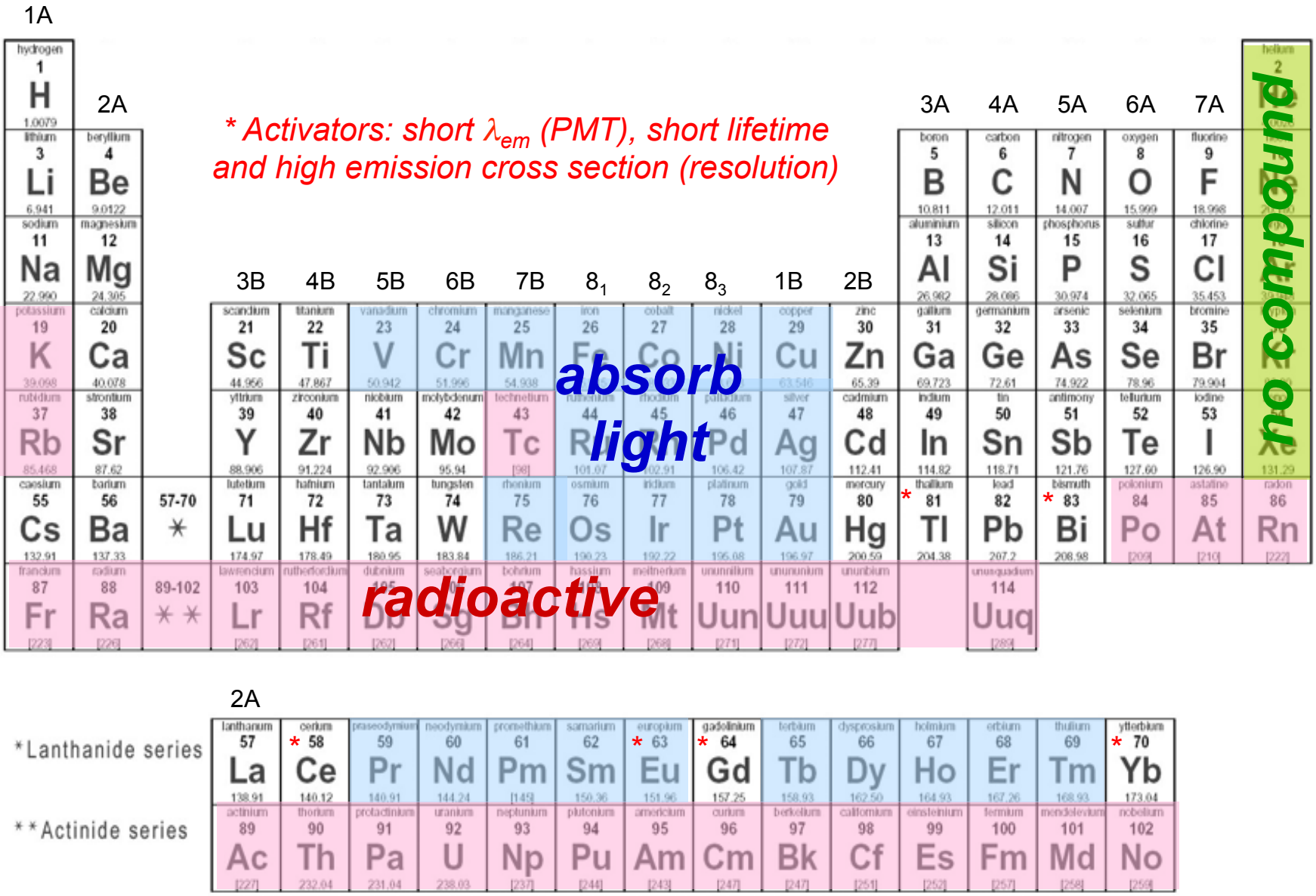

Combinatorial optimization

Theoretical light yield

$LY=E_\gamma/2.5\ E_g$

Dorenbos, NIM ***486****, 208 (2002)*

Photoelectric attenuation length

$PAL=FM/\rho\sigma_{pe}$

Ortiz et al., Comp. Mat. Sci. ***44****, 1042 (2009).*

LY vs ratio effective mass

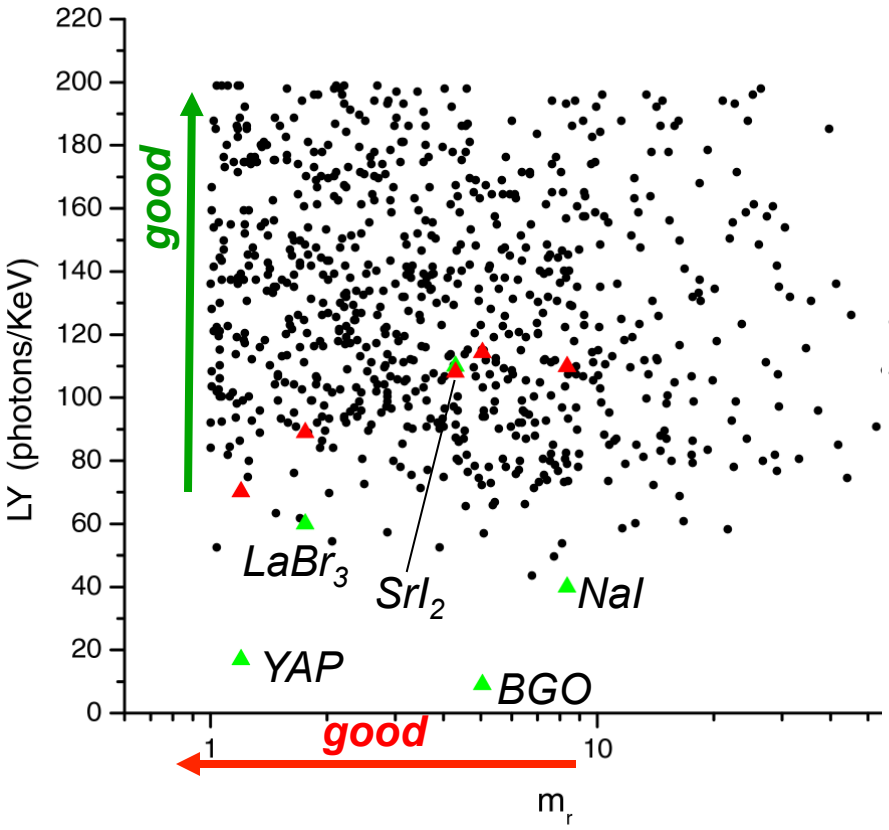

PAL vs ratio effective mass

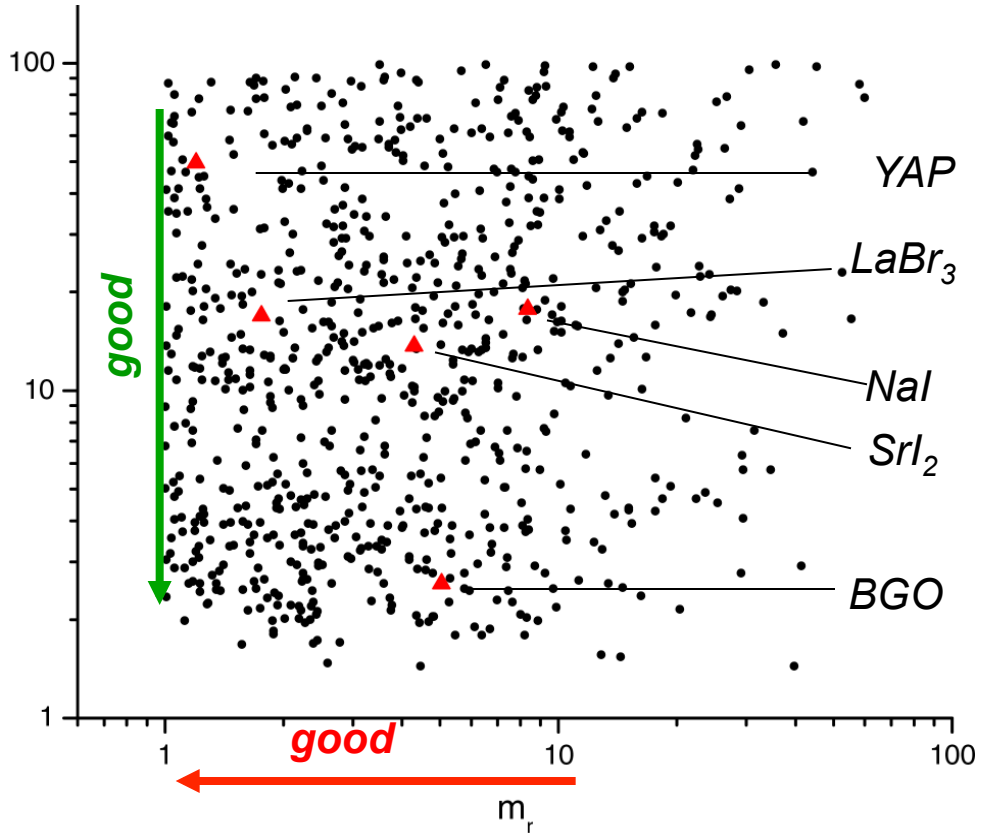

red (theoretical), green (experimental)

IEEE Trans. Nucl. Sci. ***56****, 2989 (2009).*

the Future is online

taking the bull from the horns

- Thermodynamics analysis
- Electronic structure analysis

POSTDOC OPENINGS [~many]

- **Transparent Cond.**
- **HT Corrosion**
- **Applied Math. & Information theory**

stefano@duke.edu

SPONSORS:

DOD, DOE, NIST, OSTP, DHS, BYU, TERAGRID, ORNL

ACKNOWLEDGEMENTS:

G. Hart, O. Levy, W. Setyawan, R. Taylor, N. Mingo, S. Wang, Z. Wang, K. Yang, M. Buongiorno Nardelli, S. Sanvito.

Duke UNIVERSITY

end